Environmental Research 252 (2024) 118847

Contents lists available at ScienceDirect

Environmental Research

journal homepage: www.elsevier.com/locate/envres

Metabolomics in human SGBS cells as new approach method for studying adipogenic effects: Analysis of the effects of DINCH and MINCH on central carbon metabolism

Cornelius Goerdeler [a], Beatrice Engelmann [a], Alix Sarah Aldehoff [a], Alexandra Schaffert [a,2], Matthias Blüher [b,c], John T. Heiker [c], Martin Wabitsch [d], Kristin Schubert [a], Ulrike Rolle-Kampczyk [a,1,*], Martin von Bergen [a,e,f,1]

[a] Department of Molecular Toxicology, Helmholtz Centre for Environmental Research (UFZ), Leipzig, Germany
[b] Department of Endocrinology, Nephrology and Rheumatology, Faculty of Medicine, University of Leipzig, Leipzig, Germany
[c] Helmholtz Institute for Metabolic, Obesity and Vascular Research (HI-MAG) of the Helmholtz Zentrum München at the University of Leipzig and University Hospital Leipzig, Leipzig, Germany
[d] Division of Pediatric Endocrinology and Diabetes, Ulm University Medical Center, Ulm, Germany
[e] Institute of Biochemistry, Leipzig University, Leipzig, Germany
[f] German Centre for Integrative Biodiversity Research (iDiv) Halle-Jena-Leipzig, Leipzig, Germany

ARTICLE INFO

Keywords:
Plasticizer
DINCH
Obesity
Endocrine disruption
Targeted metabolomics
Adipocyte metabolism

ABSTRACT

Growing evidence suggests that exposure to certain metabolism-disrupting chemicals (MDCs), such as the phthalate plasticizer DEHP, might promote obesity in humans, contributing to the spread of this global health problem. Due to the restriction on the use of phthalates, there has been a shift to safer declared substitutes, including the plasticizer diisononyl-cyclohexane-1,2-dicarboxylate (DINCH). Notwithstanding, recent studies suggest that the primary metabolite monoisononyl-cyclohexane-1,2-dicarboxylic acid ester (MINCH), induces differentiation of human adipocytes and affects enzyme levels of key metabolic pathways. Given the lack of methods for assessing metabolism-disrupting effects of chemicals on adipose tissue, we used metabolomics to analyze human SGSB cells exposed to DINCH or MINCH. Concentration analysis of DINCH and MINCH revealed that uptake of MINCH in preadipocytes was associated with increased lipid accumulation during adipogenesis. Although we also observed intracellular uptake for DINCH, the solubility of DINCH in cell culture medium was limited, hampering the analysis of possible effects in the μM concentration range. Metabolomics revealed that MINCH induces lipid accumulation similar to peroxisome proliferator-activated receptor gamma (PPARG)-agonist rosiglitazone through upregulation of the pyruvate cycle, which was recently identified as a key driver of *de novo* lipogenesis. Analysis of the metabolome in the presence of the PPARG-inhibitor GW9662 indicated that the effect of MINCH on metabolism was mediated at least partly by a PPARG-independent mechanism. However, all effects of MINCH were only observed at high concentrations of 10 μM, which are three orders of magnitudes higher than the current concentrations of plasticizers in human serum. Overall, the assessment of the effects of DINCH and MINCH on SGBS cells by metabolomics revealed no adipogenic potential at physiologically relevant concentrations. This finding aligns with previous *in vivo* studies and supports the potential of our method as a New Approach Method (NAM) for the assessment of adipogenic effects of environmental chemicals.

Abbreviations: LOD, limit of detection; MDC, metabolism-disrupting chemical; PPARA, peroxisome proliferator-activated receptor alpha; PPARG, peroxisome proliferator-activated receptor gamma; PPP, pentose phosphate pathway; TCA, tricarboxylic acid; TZD, thiazolidinedione.

* Corresponding author. Department of Molecular Toxicology, Helmholtz Centre for Environmental Research, Permoserstraße 15, 04318, Leipzig, Germany.
E-mail addresses: cornelius.goerdeler@ufz.de (C. Goerdeler), beatrice.engelmann@ufz.de (B. Engelmann), alix-sarah.aldehoff@ufz.de (A.S. Aldehoff), alexandra.schaffert@i-med.ac.at (A. Schaffert), Matthias.Blueher@medizin.uni-leipzig.de (M. Blüher), john.heiker@helmholtz-muenchen.de (J.T. Heiker), Martin.Wabitsch@uniklinik-ulm.de (M. Wabitsch), kristin.schubert@ufz.de (K. Schubert), ulrike.rolle-kampczyk@ufz.de, ulrike.rolle-kampczyk@ufz.de (U. Rolle-Kampczyk), martin.vonbergen@ufz.de (M. von Bergen).
[1] These authors contributed equally.
[2] Institute of Medical Biochemistry, Medical University Innsbruck, Innsbruck, Austria (Current address).

https://doi.org/10.1016/j.envres.2024.118847
Received 27 November 2023; Received in revised form 20 March 2024; Accepted 31 March 2024
Available online 4 April 2024

1. Introduction

Obesity is closely associated with several metabolic disorders such as metabolic syndrome, type 2 diabetes, and cardiovascular diseases (Gepstein and Weiss, 2019; Guh et al., 2009). Given its steadily increasing prevalence worldwide, obesity has evolved into a global pandemic, imposing substantial societal and health challenges (NCD Risk Factor Collaboration, 2017;2016; Visscher and Seidell, 2001). The causes of the increasing prevalence and obesity itself are not fully understood and depend on a complex interplay between genetic predisposition, and environmental and societal factors (Bell et al., 2005; Blüher, 2019). Apart from the sedentary lifestyle (Silveira et al., 2022) and the increased intake of highly processed food (Hall et al., 2019), a growing body of evidence indicates that exposure to certain chemical pollutants might promote obesity (Biemann et al., 2021; Darbre, 2017).

Non-covalently bound plastic additives represent an important group of chemical pollutants due to the increasing production and use of plastic products, resulting in ubiquitous human exposure. Among the most commonly used plastic additives are plasticizers, which can account for up to 35% of the weight of the plasticized material (Hennebert, 2022). Several studies suggest that exposure to plasticizers is linked to the progressive increase in non-communicable diseases, including obesity, attributed to their metabolism-disrupting properties (Meeker et al., 2009; Radke et al., 2019; Völker et al., 2022). These plasticizers are thus classified as metabolism-disrupting chemicals (MDCs) termed obesogens or adipogenic chemicals (Biemann et al., 2012; Heindel et al., 2017; Hurst and Waxman, 2003; Pomatto et al., 2018).

Phthalates are the most widely used plasticizers, accounting for more than 55% of the global plasticizer consumption in 2020 (S&P Global, 2021). Obesogenic properties have been suggested for MEHP, being the primary metabolite of the ubiquitously prevalent phthalate plasticizer DEHP. In particular, *in vitro* studies have shown that MEHP can induce adipocyte differentiation and lipid accumulation in 3T3-L1 cells (Feige et al., 2007). Similarly, *in vivo* studies have demonstrated that exposure to DEHP can induce adipogenesis, increased body weight, and impaired adipose tissue function in mice (Hao et al., 2012; Klöting et al., 2015). Analysis of the mode of action in adipocyte cell culture revealed that phthalates induce adipocyte differentiation and increase lipid accumulation by modulating hormone receptors of the nuclear receptor family such as the master regulator of adipogenesis, PPARG (Feige et al., 2007; Hurst and Waxman, 2003; Schaffert et al., 2022).

Further evidence supporting the role of phthalates in obesity development is provided by epidemiological studies showing that exposure to phthalate metabolites is associated with an elevated risk of developing obesity and insulin resistance. (Kim et al., 2016; Stahlhut et al., 2007; Wu et al., 2020). However, despite this evidence, the exact role of phthalates in the development of obesity and their mode of action remains poorly understood.

Due to their reproductive toxicity, DEHP and other phthalates have been banned in the EU for specific applications in plastic materials since 1999 (EU Commission, 1999). The plasticizer DINCH has been introduced as an alternative, especially for use in sensitive areas such as toys and medical devices. However, it was reported that the primary metabolite of DINCH, MINCH, induces adipogenesis in the stromal vascular fraction of rats (Campioli et al., 2015). In addition, global proteome analysis revealed that by activating PPARG, MINCH induces adipogenesis, alters extracellular matrix components, and affects key enzymes of central metabolic pathways in human SGSB adipocytes (Schaffert et al., 2022). In contrast, no weight-promoting properties of DINCH were observed in a two-generational study, repeated dose toxicity studies, and a combined chronic and carcinogenicity study performed in Wistar rats according to OECD guidelines (Harmon and Otter, 2022; Langsch et al., 2018). Nevertheless, specific regulatory *in vitro* and *in vivo* tests for the identification of metabolism-disrupting properties such as the promotion of adipogenesis are currently lacking (Braeuning et al., 2023). This indicates the need for the development of New Approach Methodologies (NAMs) (Schmeisser et al., 2023), to further assess potential adipogenic effects of DINCH and its metabolite MINCH.

Analyzing changes in metabolite levels by metabolomics provides a versatile tool for *in vitro* toxicology because the metabolome is highly reflective of the molecular phenotype and sensitive to perturbations by external factors (Ramirez et al., 2013; Schmeisser et al., 2023). In particular, applying metabolomics to analyze the central carbon metabolism of human adipocytes presents a potential *in vitro* method to assess adipogenesis-promoting effects, serving as a direct measure of metabolic disruption.

So far, little is known about whether and how DINCH and its metabolite MINCH influence metabolites of adipocyte key metabolic pathways. Thus, we investigated the effects of DINCH and MINCH on central carbon metabolism. The human SGBS preadipocyte cell line (Wabitsch et al., 2001) was exposed to varying amounts of each chemical. We measured concentrations by analyzing intra- and extracellular levels to draw conclusions about the uptake and potential transformation of DINCH and MINCH by the cells. Changes in the central carbon metabolism and insulin response upon exposure were assessed by targeted metabolomics. To identify potential PPARG-independent effects, SGBS cells were treated with the PPARG inhibitor GW9662.

2. Materials and methods

The plasticizer diisononyl-cyclohexane-1,2-dicarboxylate (DINCH) was purchased from abcr (CAS no. 166412-78-8, Cat.No. AB440048, 98% purity; Karlsruhe, Germany). Its primary metabolite mono-isononyl-cyclohexane-1,2-dicarboxylate (MINCH) and the secondary metabolites cyclohexane-1,2-dicarboxylic acid monocarboxyisooctyl ester (cx-MINCH), cyclohexane-1,2-dicarboxylic acid mono(hydroxy-isononyl) ester (OH-MINCH), and cyclohexane-1,2-dicarboxylic acid mono(oxo-isononyl) ester (oxo-MINCH) were obtained from Toronto Research Chemicals (Cat.No. C987305, 95% purity; C987315, 96% purity; H949710, 98% purity; and M329200, 97% purity; Toronto, ON, Canada). Information on the synthesis and exact isomer composition of DINCH was not disclosed by the manufacturer. The 4-methyloctyl isomer of MINCH, which has been identified as the most abundant isomer of DINCH (Koch et al., 2013), was used for all cell culture experiments.

2.1. Quantification of DINCH and primary and secondary metabolites

To quantify DINCH, MINCH, and the secondary metabolites in the cell culture medium and cell lysates, an adapted method by Schütze et al. (2012) was used. Note that this LC-MS/MS-based method does not allow to differentiate between the different isomers of DINCH and MINCH. For the preparation of 100 mM standard stock solutions, DINCH, MINCH, and the secondary metabolites were dissolved in MeOH. Further dilutions for a standard concentration series (100 μM, 50 μM, 25 μM, 10 μM, 7.5 μM, 5 μM, 2.5 μM, 1 μM, 750 nM, 500 nM, 250 nM, 100 nM, 10 nM, 1 nM and 0.1 nM) were prepared in 50% MeOH. To determine the absolute concentrations of DINCH, MINCH, and the secondary metabolites in the supernatant of the medium, an external calibration curve was prepared with extracted conditioned cell culture medium. The medium was conditioned with 25 μM, 10 μM, 7.5 μM, 5 μM, 2.5 μM, 1 μM, 750 nM, 500 nM, 250 nM, 100 nM, 10 nM, 1 nM and 0.1 nM of the respective substance. The intracellular concentrations were approximated using an external calibration curve with extracted cell lysate conditioned with DINCH, MINCH, or the secondary metabolites. Specifically, 20 μL of the respective chemical at different concentrations (100 μM, 50 μM, 25 μM, 10 μM, 5 μM, 1 μM, 500 nM, 100 nM, 10 nM, and 1 nM) were added to the amount of cell lysate present in a 6-well plate (approx. 20 μL).

The cell lysates for the quantification of DINCH, MINCH, and the secondary metabolites were obtained from the treatments described in 2.2 and prepared according to section 2.4.1. In brief, the treated cells

were washed twice with 0.9% (w/v) ice-cold NaCl and collected with a cell scraper. Cell lysates, supernatants (300 μL), and standard solutions (300 μL of conditioned medium or 40 μL conditioned cell lysate) were extracted with chloroform:MeOH:water (1:1:1) as described in 2.4. MEHP was used as an internal standard to account for differences in extraction efficiency. Quantification was performed after evaporation of 300 μL of the obtained non-polar phase to complete dryness and dissolving first in 35 μL MeOH, then adding 35 μL H_2O.

Extracted samples were measured on an LC-MS/MS system using an Agilent 1290 II infinity UPLC system (Agilent Technologies Inc., Santa Clara, CA, USA) for chromatographic separation coupled to a QTRAP® 6500+ system (AB Sciex, Framingham, USA) for mass spectrometric data acquisition. The following MS-related parameters for the instrument were used: Curtain Gas 40 psig, IonSpray Voltage ± 4.5 kV, Source Temperature 400 °C, Ion Source Gas 1 60 psig, and Ion Source Gas 2 40 psig.

LC separation of DINCH and MINCH was performed with different LC-gradients of solvent A (0.05% formic acid in water) and solvent B (0.05% formic acid in acetonitrile), after injecting 10 μL of sample onto a Chromolith® Performance RP-18e (2.0 × 100 mm, 1.5 μm, 130 Å; Merck, Darmstadt, Germany). For the measurement of DINCH, a 1 min equilibration with 20% B (flow rate of 0.4 mL/min) was followed by a 2-step linear increase to 50% B at 2.5 min and 95% B at 4.5 min, followed by 7.5-min isocratic elution (4.5–12 min, 0.6 mL/min flow rate) and a 2 min re-equilibration (13–15 min, 0.4 mL/min flow rate) after decrease to 20% B at 13 min. To measure MINCH, the 2-step linear increase was modified (50% B at 2.5 min and 95% B at 6.5 min) followed by a shortened 3.5 min isocratic elution (6.5–10 min, 0.6 mL/min flow rate) and a 2 min re-equilibration (11–13 min, 0.4 mL/min flow rate) after decrease to 20% B at 11 min. The temperature of the autosampler and column oven were set to 8 °C and 40 °C, respectively.

For detection and quantification, a scheduled MRM method measured in positive (DINCH) and negative (MINCH) ESI ionization mode was used. The specific transitions for the qualifier and quantifier ion of each analyte are displayed in Supplementary Table 1. The limit of detection (LOD) and limit of quantification (LOQ) values for each analyte were calculated according to the blank-based approach (Little, 2015) and are displayed in Supplementary Table 2.

2.2. SGBS cell cultivation

To study the effects of the plasticizer DINCH and its primary metabolite MINCH on adipocyte differentiation and metabolism, the human Simpson-Golabi-Behmel syndrome (SGBS) preadipocyte cell strain was used as a human adipocyte model system (Wabitsch et al., 2001). The SGBS cells were obtained from Prof. Martin Wabitsch's laboratory and cultivated in 0F medium (DMEM/F12 cell medium (1:1) containing 33 μM biotin, 17 μM pantothenate, 100 μg/mL streptomycin, and 100 IU/mL penicillin) with 10% FCS (Gibco, Carlsbad, CA, USA) at 37 °C and 5% CO_2 in 95% humidity. Cultivation was carried out in cell culture products from TPP (Trasadingen, Switzerland) and Sarstedt (Nümbrecht, Germany). TPP and Sarsted confirmed that their cell culture products are plasticizer-free.

SGBS cells were maintained and differentiated according to the standard protocol described previously (Wabitsch et al., 2001). Briefly, SGBS preadipocytes (generation 42; passage 4 after thawing) were seeded onto the respective plates and grown to confluence. Differentiation was induced by adding QuickDiff medium (serum-free 0F medium supplemented with 2 μM rosiglitazone, 25 nmol/L dexamethasone, 0.5 mmol/L 3-isobutyl-1-methylxanthine, 0.1 μmol/L cortisol, 0.01 mg/mL transferrin, 0.2 nmol/L triiodothyronine, and 20 nmol/L human insulin). After 4 days, the medium was exchanged with 3FC medium (serum-free 0F medium supplemented with 0.1 μmol/L cortisol, 0.01 mg/mL transferrin, 0.2 nmol/L triiodothyronine, and 20 nmol/L human insulin) and cells were differentiated until day 12 or day 18 after induction.

To assess the effects of DINCH and MINCH on adipogenesis, SGBS preadipocytes were cultivated in 6-well plates and treated for 12 days with differentiation media without the PPARG agonist rosiglitazone supplemented with DINCH or MINCH at concentrations of 10 nM, 100 nM, 1 μM and 10 μM. SGBS cells were differentiated in the presence of rosiglitazone to obtain an adipogenesis reference and in the absence of rosiglitazone to obtain an undifferentiated control. To control for the effects of the vehicle solvent, MeOH and DMSO were added to a final concentration of 0.01% (v/v) and 0.02% (v/v), respectively to all differentiation media. The cell culture medium was exchanged every second day, to mimic continuous exposure.

To study the effects of DINCH and MINCH on the insulin response of treated SGBS preadipocytes, an in-house MS-based insulin-dependent glucose uptake assay was performed. For the treatment of preadipocytes, SGBS cells were exposed from day 0 to day 18 in 24-well plates with differentiation media without rosiglitazone supplemented with DINCH (10 nM or 10 μM) or MINCH (10 nM or 10 μM). The extended differentiation procedure until day 18 was chosen to minimize the differentiation differences between rosiglitazone and MINCH treatment (MINCH 10 μM treatment 77% lipid accumulation of rosiglitazone-differentiated cells; Supplementary Figure 7), thereby allowing a better comparison of insulin responses.

For insulin stimulation of cells on day 18, the medium was replaced on day 17 with differentiation medium without insulin. After overnight incubation, cells were glucose starved for 1 h with 3FC medium without glucose and insulin and subsequently stimulated for 30 min with 3FC medium with insulin (stimulated cells) or without insulin (unstimulated control).

To examine the effects of DINCH and MINCH independent of PPARG, SGBS cells were exposed to differentiation media without rosiglitazone supplemented with DINCH (10 μM) or MINCH (10 μM) and together with 10 μM of the PPARG antagonist GW9662 from day 0 to day 12 in 6-well plates. The antagonist was added 1 h before adding the chemical and due to its short half-life exchanged every 2 days (Li et al., 2011), to irreversibly block PPARG before treatment. DINCH and MINCH co-treatments with GW9662 were compared to cells co-treated with rosiglitazone (d0-d4) and 10 μM GW9662 and control cells treated with 10 μM GW9662 only. All cell culture experiments were performed in quadruplicates (n = 4) or quintuplicates (n = 5).

2.3. Lipid staining

To assess lipid accumulation in SGBS cells after treatment, Oil Red O staining and DAPI/Nile red staining were used as described previously (Schaffert et al., 2022).

Briefly, cells were washed with PBS and fixed with 4% formaldehyde for 3 h at RT. After removing the formaldehyde solution, cells were again washed with PBS and the background fluorescence was recorded at 360/485 nm (E_x/E_m) for DAPI and 485/530 nm (E_x/E_m) for Nile red in a 7x7 or 11x11 spot pattern (24-well and 6-well plate, respectively) on a *Synergy*™ HT plate reader (BioTek, Winooski, VT, USA). Subsequently, the cells were stained with 1 μg/mL DAPI, 1 μg/mL Nile red, and 0.2% (w/v) saponin in PBS for 15 min. After washing three times with PBS, the fluorescence was recorded at the aforementioned wavelengths. The non-polar lipid concentration (Nile red fluorescence) is expressed as averaged relative fluorescence units (RFU) in % to control.

Following quantification of lipids *via* fluorescence measurement, fixed cells were stained with filtered Oil Red O working solution (0.1% w/v in 40% isopropanol) for 30 min at RT and washed three times with PBS. Images of stained cells in PBS were taken using a VisiScope® IT415 PH connected to a VisiCam® P6 digital camera (VWR, Radnor, PA, USA) at 10 × magnification.

2.4. Extraction of central carbon metabolites

2.4.1. Intracellular metabolites

To analyze the intracellular concentrations of central carbon metabolites in SGBS cells a MeOH/chloroform/water (1:1:1) extraction was performed. Before extraction, SGBS cells were washed twice by removing the cell medium and adding 2 × 1 mL 0.9% ice-cold NaCl. After removing the NaCl solution, metabolism was quenched by adding MeOH (−20 °C) with 100 nM MEHP (internal standard DINCH/MINCH measurement) and ice-cold H_2O with 10 μM d6-glutarate (internal standard for central carbon metabolites) to the cells in equal amounts (400 μL for 6-well plates, 200 μL for 24-well plates). The cells were collected by a cell scraper and transferred into a new 2 mL tube with chloroform (−20 °C, 400 μL for 6-well plates, 200 μL for 24-well plates). After shaking at 1.400 rpm and 4 °C for 20 min, the extraction mixture was centrifuged at 18,000 g and 4 °C for 5 min. Subsequently, the polar (central carbon metabolites) and non-polar fraction (DINCH/MINCH quantification) were collected (300 μL for 6-well plate, 250 μL for 24-well plate) and evaporated to complete dryness (Concentrator plus, Eppendorf, Hamburg, Germany). The metabolite pellets were stored at −80 °C until further analysis. For measurement, pellets of the polar fraction were re-dissolved in 100 μL water, whereas pellets of the non-polar fraction were re-dissolved in 35 μL MeOH, followed by adding 35 μL H_2O.

2.4.2. Extracellular metabolites

Extracellular metabolites in the medium were extracted by MeOH/chloroform/water (1:1:1) extraction. Following treatment, 1 mL medium from each condition was collected and centrifuged at 10,000 g and 4 °C for 10 min. After transferring 300 μL of the supernatant into a new tube, the metabolites were extracted by adding 400 μL MeOH (−20 °C) with 100 nM MEHP, 100 μL ice-cold H_2O with 40 μM d6-glutarate and 400 μL chloroform (−20 °C). The extraction mixture was shaken at 1.400 rpm and 4 °C for 20 min and subsequently centrifuged for 10 min at 18,000 g and 4 °C. The polar and non-polar fractions were collected (300 μL for 6-well plates, 250 μL for 24-well plates) and evaporated to complete dryness in an Eppendorf® Concentrator plus. The obtained pellets were stored at −80 °C until further analysis. Before measurement, pellets of the polar fraction were re-dissolved in 100 μL water and pellets of the non-polar fraction were re-dissolved in 35 μL MeOH, followed by adding 35 μL H_2O.

2.5. Targeted mass spectrometry analysis of central carbon metabolites

Extracted intra- and extracellular central carbon metabolites of SGBS cells were analyzed by LC-MS/MS using an adapted method described by Buescher et al. (2010). For the chromatographic separation and the mass spectrometric data acquisition, the same devices as in 2.1 were used. Initially, 10 μL of the resuspended sample were injected onto an XSelect HSS T3 XP column (2.1 × 150 mm, 2.5 μm, 100 Å; Waters, Milford, MA, USA) connected to an XP VanGuard® cartridge (HSS T3, 2.1 × 5 mm, 2.5 μM; Waters, Milford, MA, USA). Metabolites were eluted at a flow rate ranging from 0.4 mL/min to 0.15 mL/min with a non-linear gradient as described in Supplementary Table 3. Mobile phase A and phase B were composed of 10 mM tributylamine, 10 mM acetic acid, 5% methanol, 2% 2-propanol (pH 7.2), and 100% 2-propanol, respectively. The autosampler was kept at 8 °C and the temperature of the column oven was set to 40 °C.

Data acquisition and analysis were performed with the Analyst® software version 1.7.1 and Sciex OS version 1.6.1, respectively. Identification and quantification were based on specific MRM transitions measured in negative ESI mode. The selected MRM transitions for the analysis of central carbon metabolites are provided in Suppl Table 4.

2.6. Metabolite abundance normalization

Intracellular and extracellular metabolite abundances were normalized to the DAPI-stained DNA content per well (DAPI fluorescence) measured in additional wells on the respective treatment plate. The normalization wells were seeded together with the cell plates for extraction using the same seeding concentration. On the day of extraction, the cells of the normalization plate were fixed with 4% formaldehyde solution and stained with DAPI according to the described DAPI/Nile Red staining protocol. The normalization factor was calculated by dividing the mean DAPI RFU of each treatment by the total mean DAPI RFU of all treatments. If not otherwise mentioned, four replicates (n = 4) were used for each treatment. After normalization, log2 fold changes of the respective treatments (DINCH, MINCH, or rosiglitazone) compared to the control cells were calculated by dividing the normalized peak area obtained from each replicate to the respective control (Log2FC values for treatment without inhibitor: Supplementary Tables 5 and 6; for treatment with inhibitor: Supplementary Table 8). For the analysis of the data from the insulin response experiment, no DAPI normalization was performed because the fold change was calculated by dividing the intensities of the insulin-stimulated cells with the non-stimulated cells of each treatment (plus *vs*. minus; fold changes in Supplementary Table 7).

2.7. Statistical analysis

GraphPad Prism software (Version 10.0, La Jolla, CA, USA) and R software (Version 4.05) were used for visualization and statistical analysis. For the statistical analysis of the lipid accumulation, a one-way ANOVA test followed by Dunnett's post-hoc test was performed against the untreated control. Statistical analysis of metabolite abundances was performed by a Welch ANOVA test followed by a Games-Howell post-hoc test. Outliers in the metabolite abundance data were removed after performing a Grubbs outlier test with $\alpha = 0.05$ in GraphPad Prism. If not otherwise noted, data are represented as means ± standard deviation (SD). Heatmaps were created with an R script using the basic functions and the reshape, ggplot, and scales packages. The PCA and calculation of the PERMANOVA were performed in R using the basic functions and the vegan package.

3. Results

3.1. Analysis of extra- and intracellular concentrations of DINCH and MINCH

To assess any disparities between the nominal concentrations of DINCH and MINCH used in the *in vitro* system and their actual concentrations, as well as to track concentration changes over time, the cell culture conditioned medium was analyzed for DINCH and MINCH. For this purpose, DINCH and MINCH (10 nM, 100 nM, 1 μM, and 10 μM) conditioned medium was measured before last treatment (on day 10) and 48 h after treatment of SGBS cells (on day 12). The measured concentrations of MINCH before treatment were in good agreement with the applied concentrations (72–119% of applied dose; Fig. 2A, Supplementary Figure 1). In contrast, only a fraction of the nominal applied concentrations of DINCH were detected (4–8% of applied dose; Fig. 2A, Supplementary Figure 1), which was expected due to its hydrophobic properties (log K_{ow} 9.8). For clarity, nominal concentrations are used in the following to distinguish between treatments.

After incubation for 48 h, a notable decrease in the measured concentration of DINCH was observed in the medium. There was a 2.8-fold and 5.2-fold reduction for 1 μM and 10 μM, respectively. Similarly, MINCH also showed a decrease ranging from 1.9 to 2.5-fold across all applied concentrations (Fig. 2A, Supplementary Figure 1). To verify that this finding was at least partially due to cellular uptake, we extracted SGBS cells after stringent washing on day 12 of treatment. It should be noted that despite stringent washing steps to remove extracellularly

bound chemicals before analyzing the cell lysates, it cannot be excluded that part of the measured DINCH or MINCH was bound extracellularly to the cell membrane. Thus, the term intracellular also includes potentially extracellularly bound chemicals. Indeed, both DINCH and MINCH were detected in the cell lysates with nearly linear increasing concentrations from the 10 nM to the 10 μM treatment (Fig. 2B). Noteworthy, even at the 10 nM treatment, DINCH was detected intracellularly, although the measured concentration in the conditioned medium was below the limit of detection (LOD).

Since the biotransformation of phthalates has been observed in various *in vitro* systems e.g. human mononuclear cells (Hansen et al., 2015), thyroid epithelial cells (Frohnert Hansen et al., 2016), and testis explants (Desdoits-Lethimonier et al., 2012), the metabolization of DINCH to MINCH and its secondary metabolites, oxo-MINCH, OH-MINCH, and cx-MINCH, was analyzed in SGBS cells.

Therefore, MINCH levels were assessed in the cell culture medium containing the highest applied DINCH concentration (nominal concentration of 10 μM) before and 48 h after treatment of SGBS cells on day 10. These measurements were compared to DINCH-containing medium incubated under abiotic conditions for 48 h and 96 h. The cell culture medium before incubation contained low concentrations of MINCH (0.5 nM, Fig. 2A), which is in line with the measurement of MINCH in a 10 μM DINCH stock solution in MeOH (data not shown).

After 48 h, an almost 10-fold increase in MINCH concentration was detected in the medium incubated with SGBS cells (mean concentration: 4.8 nM), but not in the medium incubated under abiotic conditions (Fig. 2A). Significant reductions in MINCH abundance were observed in the medium incubated under abiotic conditions for 48 h and 96 h. This decrease in MINCH levels is likely attributed to the absorption onto the walls of the culture plates, which are made of polystyrene (Dimitrijevic et al., 2022). Further analysis of MINCH in cell lysates of SGBS cells treated with 10 μM DINCH for 12 days showed that MINCH was detected intracellularly at a concentration of 2.4 pmol/cell × 10^6, which is equivalent to treating SGBS cells with approximately 37 nM MINCH for 12 days (Fig. 1B, Fig. 2B). Again, comparison with cell culture plates extracted at 48 h and 96 h without cells confirmed that the metabolization of DINCH to MINCH is cell-dependent (Fig. 2B). Further cell-dependent biotransformation of MINCH to the secondary oxidized metabolites of DINCH, namely oxo-MINCH, OH-MINCH, and cx-MINCH, was not observed after incubation with DINCH conditioned medium (intensities below LOD). However, low levels of OH-MINCH (1.5 nM) were detected 48 h after treatment with 10 μM MINCH-conditioned medium of SGBS cells on day 10 (Supplementary Figure 2). Furthermore, analysis of the cell lysate of SGBS cells treated with 10 μM MINCH for 12 days revealed that OH-MINCH could be detected at a low concentration of 0.01 pmol/cell × 10^6, but not oxo-MINCH or cx-MINCH (Supplementary Figure 2).

In summary, concentration analysis of the supernatant and internal cell load revealed that the concentration of DINCH and MINCH in cell culture medium decreased after cell incubation, which was accompanied by a nearly linear uptake of DINCH and MINCH. In addition, the data show that the solubility of DINCH is limited to about 500 nM in the cell culture medium. The detection of MINCH in DINCH-treated SGBS cells and of OH-MINCH in MINCH-treated SGBS cells, but not under abiotic conditions, demonstrates the ability of biotransformation by SGBS cells.

3.2. *Effects of DINCH and MINCH on adipocyte metabolism*

After the confirmation of cellular uptake of DINCH and MINCH, we investigated the effects on major adipocyte metabolic pathways in light of prior findings regarding the effects of MINCH on key enzymes of adipocyte central carbon metabolism (Schaffert et al., 2022). The intracellular metabolite abundances of metabolites involved in glycolysis, pentose phosphate pathway (PPP), tricarboxylic acid (TCA) cycle, and associated amino acids (Supplementary Figure 3) were measured in SGBS cells after 12 days of continuous treatment with DINCH or MINCH (10 nM–10 μM). The lowest concentration of 10 nM was selected

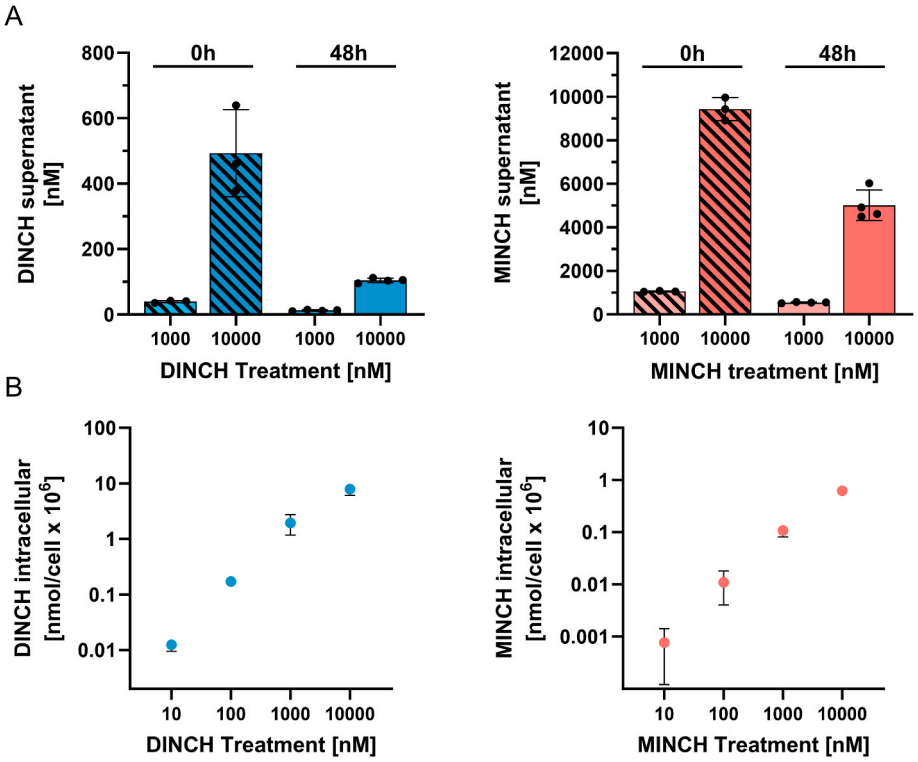

Fig. 1. Analysis of extra- and intracellular concentrations of DINCH and MINCH. (A) DINCH and MINCH concentrations (1 μM and 10 μM nominal treatment concentration) in medium supernatant before and 48 h after SGBS treatment on day 10 (n = 3–4). (B) Intracellular concentrations of DINCH and MINCH after 12 days of SGBS cell treatment (n = 4). Data are presented as absolute concentrations in [nM] (A) or [nmol/cell × 10^6] (B), and values are expressed as mean ± SD.

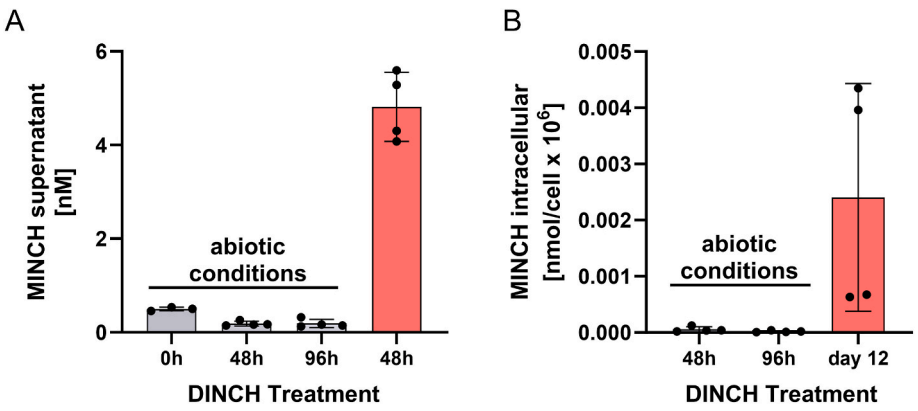

Fig. 2. Biotransformation of DINCH in SGBS cells. (A) Concentration of MINCH in 10 μM DINCH medium 48 h after treatment of SGBS cells on day 10 compared to 10 μM DINCH medium incubated for 0 h, 48 h, and 96 h under abiotic conditions (n = 3–4). (B) Intracellular concentrations of MINCH after 12 days of treatment of SGBS cells with 10 μM DINCH (n = 4) compared to cell culture plates extracted 48 h and 96 h after incubation with 10 μM DINCH under abiotic conditions. Data are presented as absolute concentrations in [nM] (A) or [nmol/cell × 10^6] (B) and values are expressed as mean ± SD.

because it corresponds to the concentrations of phthalate plasticizers in human serum (Axelsson et al., 2015; Frederiksen et al., 2010), which were considered since concentrations of DINCH in human serum have not yet been published. Metabolite levels of treated cells were compared to SGBS cells differentiated with rosiglitazone and untreated control cells.

Analysis of lipid accumulation prior to metabolite analysis confirmed the adipogenic potential of MINCH in the μM concentration range, which is consistent with the results previously described (Schaffert et al., 2022). On day 12 of treatment, neither DINCH nor the 10 nM–100 nM concentration of MINCH induced lipid accumulation of SGBS cells (Supplementary Figure 4). In contrast, 1 μM MINCH slightly (117% of Ctrl) and 10 μM MINCH more strongly (141% of Ctrl) induced lipid accumulation, albeit at a lower level compared to preadipocytes differentiated with rosiglitazone (216% of Ctrl; Supplementary Figure 4).

Intracellular metabolite levels showed that the DINCH treatments and the low MINCH concentrations (10 nM and 100 nM) were closely grouped to control cells, whereas the 10 μM MINCH treatment and rosiglitazone-differentiated cells were significantly separated from the control (Fig. 3A). However, the cells treated with 10 μM MINCH were grouped closer to the control cells than to the cells differentiated with rosiglitazone. Similar to the 10 μM MINCH treatment, the 1 μM MINCH treatment showed separate clustering from the control group, but to a lesser extent, and the group distance was not significant (Fig. 3A).

Analysis of metabolic changes at the pathway level revealed that rosiglitazone-differentiated cells showed the most significant changes compared to control cells, followed by the 10 μM MINCH treatment, while the other treatments showed little or no effect (Fig. 3B). Metabolite levels of upper (reactions from glucose to glyceraldehyde 3-phosphate (G3P): hexokinase (HK), phosphoglucose isomerase (PGI), phosphofructokinase-1/2 (PFK1/2), aldolase (ALDO) and triosephosphate isomerase (TIM)) and lower glycolysis (reactions from G3P to pyruvate: glyceraldehyde 3-phosphate dehydrogenase (GAPDH), phosphoglycerate kinase (PGK), phosphoglycerate mutase (PGM), enolase (ENO) and pyruvate kinase (PK)) were strongly elevated in rosiglitazone-differentiated cells with the highest increase observed for glycerol 3-phosphate (Gro3P) levels. While no changes were observed in upper glycolysis by treatment with 10 μM MINCH, metabolites of lower glycolysis were significantly elevated, similar to rosiglitazone-differentiated cells. Again, the strongest increase was observed for Gro3P and G3P (Fig. 3B).

As observed for glycolysis, PPP metabolites were strongly elevated in rosiglitazone-differentiated cells (Fig. 3B). In contrast, PPP concentrations were not altered by DINCH or MINCH treatment except for a slight increase in sedoheptulose 7-phosphate (100 nM–10 μM DINCH treatment, Fig. 3B).

At the metabolic junction between glycolysis to TCA, acetyl-CoA and the associated malonyl-CoA, the substrates for fatty acid synthesis, were significantly elevated in cells treated with rosiglitazone and 10 μM MINCH (except malonyl-CoA 10 μM MINCH treatment: p = 0.06; Fig. 3B and. 4).

Further downstream of acetyl-CoA, the alterations in metabolite levels within the TCA cycle of rosiglitazone-differentiated adipocytes were divided into two parts. There were no significant changes from citrate to α-ketoglutarate followed by a significant decrease in succinate and a strong significant increase from fumarate to oxaloacetate (Fig. 3B). A similar response in TCA cycle metabolites was observed in cells treated with 10 μM MINCH, although the increase in fumarate and malate was absent (Fig. 3B). Again, these changes in metabolite levels were not observed at the lower concentrations of MINCH and any used DINCH concentrations.

Pyruvate, oxaloacetate, and acetyl-CoA, along with malate, form an important metabolic junction for *de novo* lipogenesis and NAPDH production in differentiated 3T3-L1 adipocytes (Oates and Antoniewicz, 2022; Roberts et al., 2009). Changes in these metabolite levels were analyzed along with the associated enzyme levels (ATP-citrate lyase (ACLY), citrate synthase (CS), malate dehydrogenase (MDH1), malic enzyme (ME) 1 and 2, pyruvate carboxylase (PC), and pyruvate dehydrogenase (PDH)) from the published proteome data set (Schaffert et al., 2022). Consistent with the increased metabolite levels of pyruvate, oxaloacetate, and acetyl-CoA in both, rosiglitazone differentiated cells and 10 μM MINCH-treated cells, a strong induction of ACLY, PDH, PC, and CS were observed on day 12 of treatment (Fig. 4, Supplementary Figure 5). Moreover, protein levels of malate dehydrogenase and malic enzyme were significantly increased by 10 μM MINCH and rosiglitazone (Supplementary Figure 5).

However, only rosiglitazone-differentiated cells, but not cells treated with 10 μM MINCH, showed elevated metabolite levels of malate (Fig. 3B). Contrary to what was observed for 10 μM MINCH-treated and rosiglitazone-differentiated cells, treatment with DINCH and low concentrations of MINCH resulted only in a slight and inconsistent induction of enzyme levels of the pyruvate cycle and no changes in associated metabolite levels (Fig. 3B and. 4, Supplementary Figure 5).

In addition to intracellular metabolite levels, secretion and uptake of lactate and the amino acids alanine, asparagine, aspartate, glutamate, and glutamine were measured on day 12 (48 h after incubation). Whereas glutamate, glutamine, and aspartate were taken up and asparagine levels remained unchanged, alanine and lactate were secreted in all treatments, including control cells (Fig. 4, Supplementary Figure 6). For the amino acids that were consumed, the uptake was similar to the control, except for a reduced uptake of aspartate

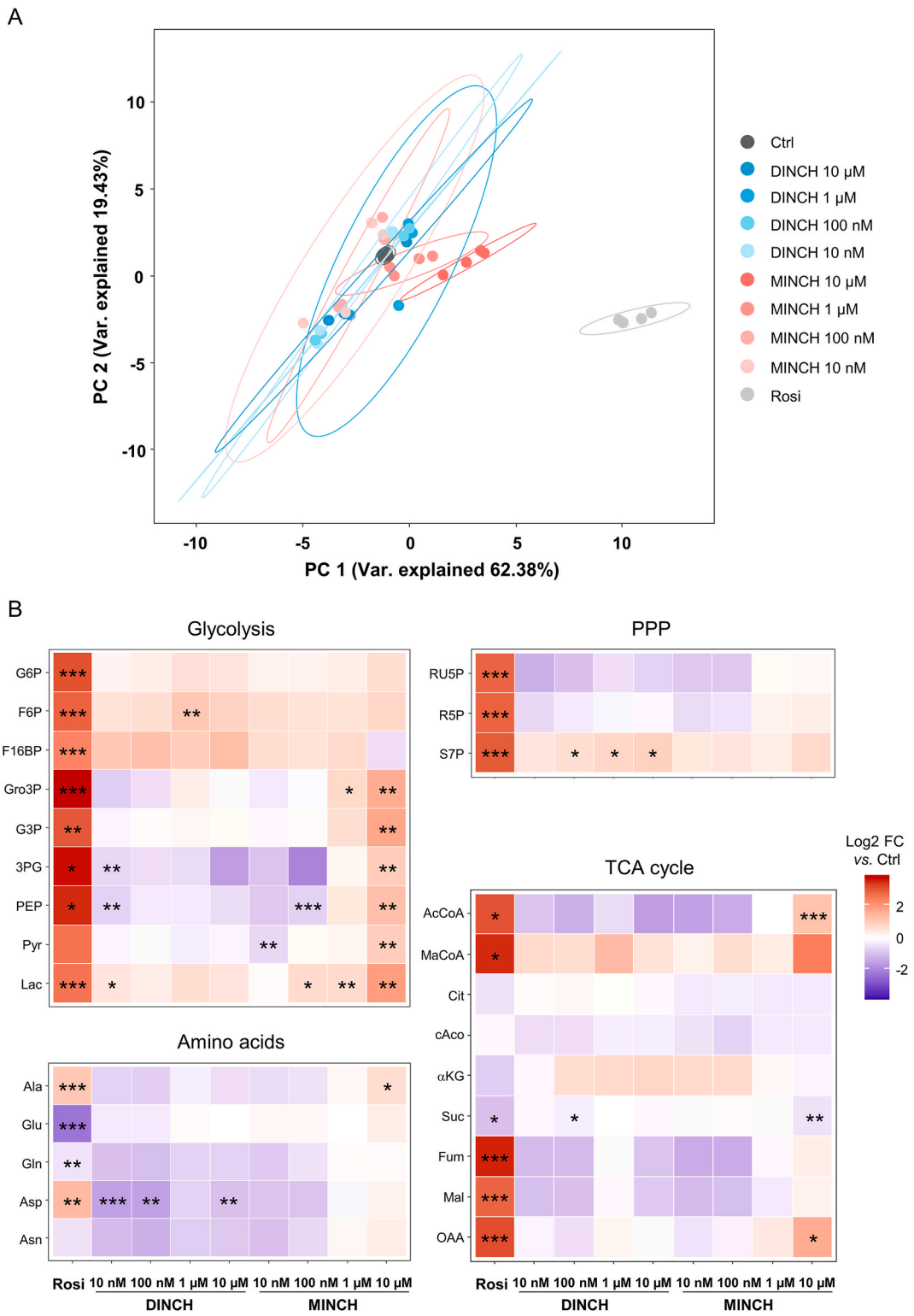

Fig. 3. Effects of DINCH and MINCH on central carbon metabolism. (A) Principal component analysis of extracted intracellular metabolites of glycolysis, PPP, TCA, and associated amino acids of SGBS cells treated for 12 days with different concentrations of DINCH or MINCH (10 nM-10 µM) and compared to rosiglitazone differentiated cells (Rosi) and control cells (Ctrl). Significances between the treatments and the control were tested by a PERMANOVA (significant distance for Rosi vs. Ctrl and MINCH 10 µM vs. Ctrl: $p = 0.032$ and $p = 0.033$, respectively). (B) Metabolite abundances of SGBS cells after 12 days of treatment with DINCH or MINCH and SGBS cells differentiated with rosiglitazone (Rosi) presented as log2 fold changes compared to the control ($n = 4$). Metabolite levels were normalized to the DNA content determined by DAPI fluorescence. Grubbs outlier test with $\alpha = 0.05$ was used to remove outliers (acetyl-CoA MINCH 10 µM). Welch ANOVA followed by Games-Howell post-hoc test was performed to calculate statistical significance; *$p < 0.05$, **$p < 0.01$, ***$p < 0.001$. AcCoA - acetyl-CoA, Ala – Alanine, Asn – asparagine, Asp – aspartate, Cit – citrate, cAco – *cis*-aconitate, Fum – fumarate, F1,6BP – fructose 1,6-bisphosphate, F6P – fructose 6-phosphate, G6P – glucose 6-phosphate, Glu – glutamate, Gln – glutamine, G3P – glyceraldehyde 3-phosphate, Gro3P – glycerol 3-phosphate, αKG – α-ketoglutarate, Lac – lactate, MaCoA – malonyl-CoA, Mal – malate, OAA – oxaloacetate, PEP – phosphoenolpyruvate, R5P – ribose 5-phosphate, RU5P – ribulose 5-phosphate, S7P – sedoheptulose 7-phosphate, Suc – succinate, 3 PG – 3-phosphoglycerate.

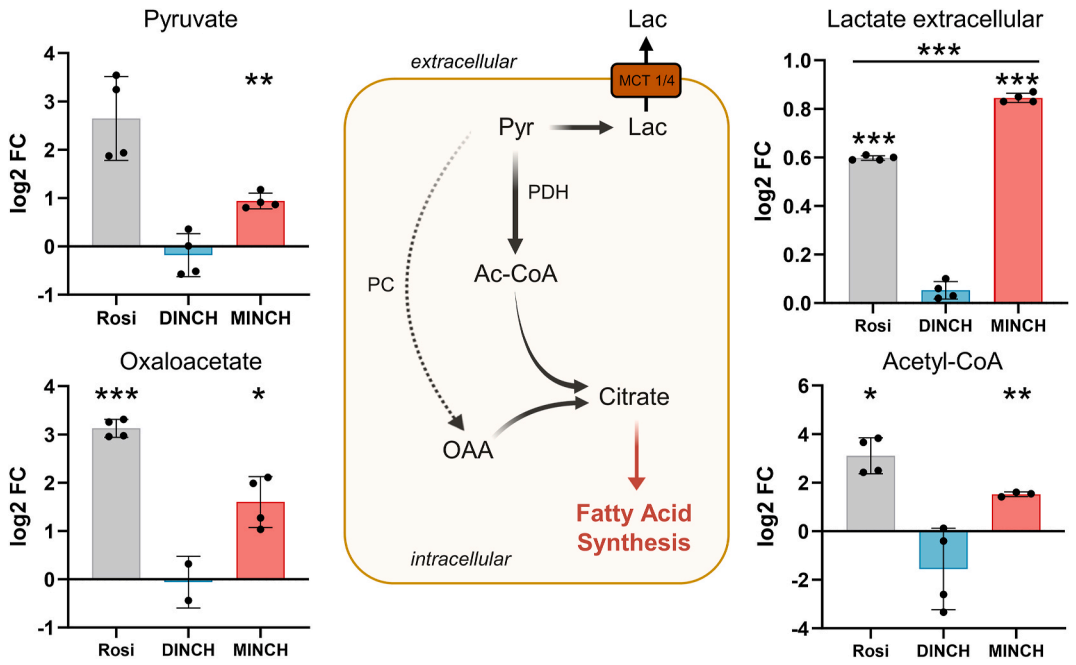

Fig. 4. Effects of DINCH and MINCH on the metabolites of the pyruvate cycle. DAPI normalized abundances of selected metabolites of the pyruvate junction of SGBS cells after 12 days of treatment with DINCH or MINCH and SGBS cells differentiated with rosiglitazone (Rosi). Data are shown as log2 fold change of the respective treatment compared to control cells and values are expressed as mean ± SD (n = 4). Grubbs outlier test with α = 0.05 was used to remove outliers (acetyl-CoA MINCH 10 μM). Statistical significance was calculated by Welch ANOVA followed by Games-Howell post-hoc test; *p < 0.05, **p < 0.01, ***p < 0.001. Ac-CoA – acetyl-CoA, Lac – lactate, MCT1/4 – monocarboxylate transporter 1 and 4, OAA – oxaloacetate, PC – pyruvate carboxylase, PDH – pyruvate dehydrogenase, Pyr – pyruvate.

(reduction was strongest with rosiglitazone, followed by MINCH; Supplementary Figure 6). Lactate and alanine as end products of glycolysis showed a significantly increased secretion in MINCH and rosiglitazone differentiated cells compared to undifferentiated control cells (Fig. 4). Interestingly, lactate secretion was even significantly higher in cells treated with 10 μM MINCH compared to cells differentiated with rosiglitazone (Fig. 4).

In summary, MINCH in the μM concentration range affected the glycolysis and the TCA cycle of SGSB cells similar to cells differentiated with rosiglitazone, although the changes in metabolite levels were less pronounced. While the effects of MINCH on the metabolome were apparent at 10 μM by significant separation of the control treatment (Fig. 3A), DINCH at concentrations investigated did not induce alterations in metabolites of the central carbon metabolism.

3.3. Insulin response of DINCH- and MINCH-treated SGBS preadipocytes

Elevated lactate production by adipose tissue and increased lactate plasma levels are associated with obesity and insulin resistance (DiGirolamo et al., 1992; Lovejoy et al., 1992). To investigate the relation between increased lactate levels observed in MINCH-treated SGBS cells and potential changes in insulin sensitivity, we analyzed the insulin response of MINCH-treated SGBS cells compared to rosiglitazone-differentiated cells. After prolonged treatment with MINCH (10 nM and 10 μM), DINCH (10 nM and 10 μM), or rosiglitazone (200 nM and 2 μM), SGSB cells were insulin starved on day 17 and stimulated with insulin for 30 min on day 18 after glucose starvation. Subsequently, metabolites were extracted to analyze changes in glycolysis and PPP in comparison to treated SGBS cells without insulin stimulation. Again, the highest accumulation of intracellular lipids was observed for rosiglitazone-treated SGBS cells, followed by 10 μM MINCH-treated cells (Supplementary Figure 7).

Although lipid accumulation was significantly lower in MINCH-treated cells compared to rosiglitazone-treated cells (1.2-fold decrease), the insulin response was almost identical for upper glycolysis and PPP compared to rosiglitazone-treated cells (Fig. 5, Supplementary Figure 8). The highest increase in rosiglitazone and MINCH-treated cells was observed for fructose 1,6-bisphosphate (FBP), consistent with literature showing that intracellular FBP concentrations correlate with glycolytic flux rate (Tanner et al., 2018). At the beginning of lower glycolysis, a similar insulin response was observed between MINCH and rosiglitazone-treated cells (Fig. 5). However, this shifted towards the lower part with PEP showing a lower fold change in MINCH-treated cells (Fig. 5). For pyruvate, no insulin response was observed (Supplementary Figure 8), which is presumably because intracellular pyruvate levels are strongly affected by the external pyruvate pool in the cell culture medium as seen for 3T3-L1 adipocytes (Oates and Antoniewicz, 2022). In contrast, further downstream, the fold changes were again increased in MINCH-treated cells for extracellular lactate levels and acetyl-CoA levels. Whereas the insulin response for secreted lactate was similar to that for rosiglitazone, the insulin response for acetyl-CoA was even significantly higher in MINCH-treated cells. As expected, contrary to the high dose of MINCH and the rosiglitazone-differentiated cells, treatment with DINCH and the low MINCH concentration showed minimal to no insulin response. This aligns with the absence of differentiation and the lack of effects on central carbon metabolites (Fig. 5, Supplementary Figures 7 and 8).

In brief, cells treated with MINCH showed a similar degree of increased insulin response of glycolysis and PPP as rosiglitazone differentiated cells. The effects were observed at the highest concentration of 10 μM MINCH, but not at the lower concentration tested and not in cells treated with DINCH.

3.4. Possible PPARG-independent effects of DINCH and MINCH

Binding studies using surface plasmon resonance spectroscopy and receptor gene assay in HEK293 cells showed that MINCH can bind and activate PPARG in the μM concentration range (Engel et al., 2018; Schaffert et al., 2022). However, it remains unclear whether the master regulator of adipogenesis, PPARG is the main target of MINCH or other

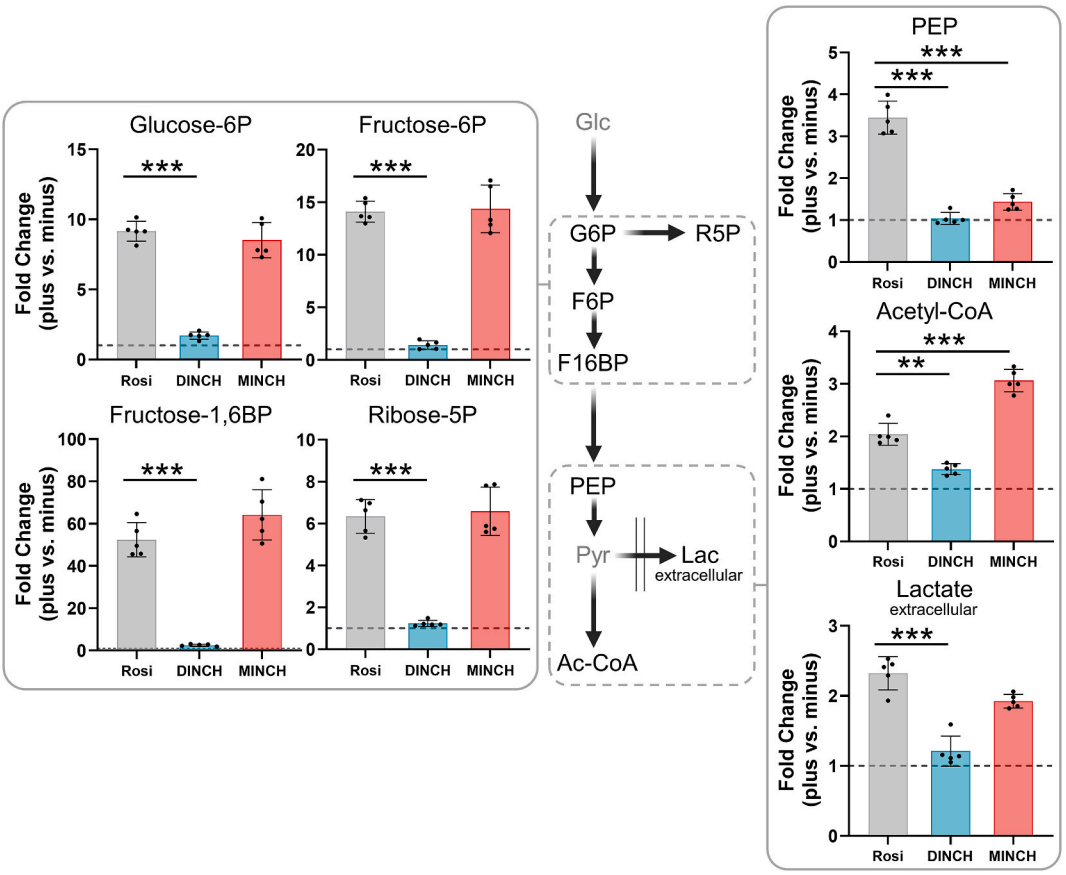

Fig. 5. Insulin response of glycolytic and PPP metabolites after DINCH and MINCH treatment. Changes of metabolite abundances of glycolysis and PPP after 30 min of insulin stimulation of SGBS preadipocytes exposed for 18 days to 10 μM DINCH, 10 μM MINCH, or differentiated with rosiglitazone. Data are shown as fold change of the insulin-stimulated cells compared to unstimulated cells of the respective treatment (plus *vs.* minus) and values are expressed as mean ± SD (n = 5). Statistical significance (DINCH and MINCH treatment *vs.* Rosi) was calculated by Welch ANOVA followed by Games-Howell post-hoc test; *p < 0.05, **p < 0.01, ***p < 0.001. Ac-CoA – acetyl-CoA, Frc-6P – fructose 6-phosphate, Frc-1,6BP – fructose 1,6-bisphosphate, Glc – glucose, Glc-6P – glucose 6-phosphate, Lac – lactate, PEP – phosphoenolpyruvate, Pyr – pyruvate, Rib-5P – ribulose 5-phosphate.

nuclear receptors play an additional important role (Schaffert et al., 2022). Thus, we aimed to elucidate the PPARG-independent effects of DINCH and MINCH on SGBS cell metabolism. SGBS preadipocytes were treated for 12 days with 10 μM MINCH or 10 μM DINCH and in the presence of 10 μM of the selective PPARG inhibitor GW9662. These were then compared to cells that received a combination treatment of rosiglitazone (2 μM) and 10 μM GW9662, and to control cells that were solely treated with 10 μM GW9662. To irreversibly block PPARG, cells were incubated with GW9662 for 1 h prior to DINCH/MINCH treatment every 2 days.

On day 12, lipid accumulation was less prominent in Rosi + GW treated cells (59% reduction compared to Rosi; Fig. 6A, Supplementary Figure 9). The same was observed for the comparison of MINCH + GW-treated cells *vs.* MINCH treatment alone (32% reduction compared to 10 μM MINCH; Fig. 6A, Supplementary Figure 9). However, cells treated with rosiglitazone or MINCH while inhibited with GW9662 still showed significantly higher lipid content than cells treated with the inhibitor and vehicle solvents only (Rosi + GW: 126% of Ctrl + GW; MINCH + GW: 117% of Ctrl + GW; Fig. 6A, Supplementary Figure 9 and 10A). DAPI staining confirmed that treatment with 10 μM of GW9662 did not affect cell viability (Supplementary Figure 10B).

Analysis of central carbon metabolism revealed that the effects on the metabolome were strongly reduced by the inhibitor as seen in Rosi + GW and MINCH + GW treatment compared to the same treatments without inhibitor (Fig. 6B). These findings were expected since PPARG is the primary mediator of adipogenesis. Nevertheless, ROSI + GW treatment showed a tendency toward elevated metabolite levels of lower glycolysis and a significant increase in PEP, indicating higher glycolytic activity (Fig. 6B). This was not observed in the DINCH + GW or MINCH + GW treatments. Strikingly, the metabolite acetyl-CoA and oxaloacetate were significantly elevated with MINCH + GW treatment, similar to the effects observed without the inhibitor on metabolites of the pyruvate cycle (Fig. 6B). A partly similar effect was observed in the Rosi + GW treatment, whereby oxaloacetate levels were significantly elevated, but not acetyl-CoA levels. In line with the results from treatment without inhibitor, the effects of DINCH + GW treatment on central carbon metabolites were negligible (Fig. 6B).

In addition to the effects on intracellular metabolites, changes in extracellular metabolites were analyzed. Lactate secretion was significantly increased in MINCH + GW treatment (Fig. 6B), as was observed in MINCH treatment without inhibitor, but not in DINCH + GW or Rosi + GW treatment.

In summary, the effects of MINCH and rosiglitazone were strongly reduced in the presence of the PPARG inhibitor GW9662. However, a slight and significant increase in lipid accumulation was observed in Rosi + GW and MINCH + GW treatment. In addition, elevated lactate secretion and increased levels of metabolites of the pyruvate cycle were consistently observed in MINCH treatment even after inhibition of PPARG. Although treatment with Rosi + GW did not show an increase in lactate secretion, a partially similar response was observed in the pyruvate cycle due to the increased oxaloacetate levels.

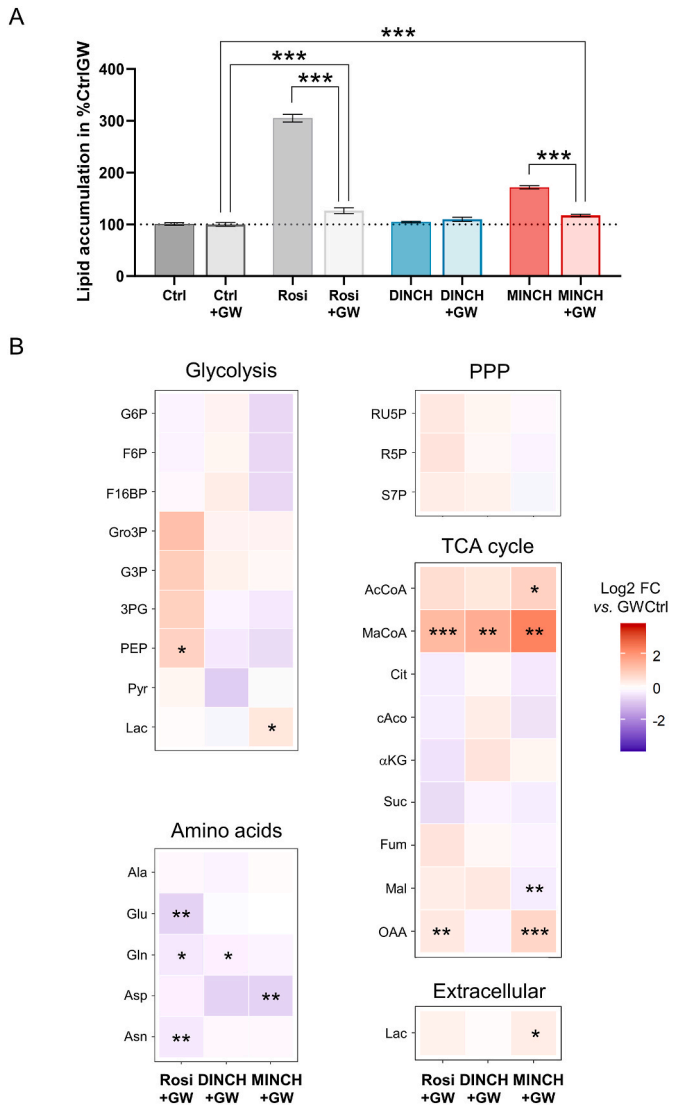

Fig. 6. PPARG independent effects of DINCH and MINCH on SGBS cells. (A) Lipid accumulation of SGBS cells after 12 days of treatment with DINCH, MINCH, or rosiglitazone in the presence of the PPAR-γ antagonist GW9662. GW9662 co-treatments (MINCH + GW, DINCH + GW, Rosi + GW, Ctrl + GW) were compared to the respective treatments without GW, and lipid content was assessed by measuring Nile red fluorescence (n = 5). (B) Intracellular metabolite abundances and extracellular lactate levels of SGBS cells after 12 days of treatment with DINCH, MINCH, or rosiglitazone (Rosi) in the presence of 10 μM GW9662 (n = 4). Metabolite levels were normalized to the DNA content determined by DAPI fluorescence. Data in (A) are presented as an increase or decrease over control (Ctrl) in % and in (B) as log2 fold changes compared to the inhibitor control (Ctrl + GW). Values are expressed as mean ± SD. Welch ANOVA followed by Games-Howell post-hoc test was performed to calculate statistical significance; *$p < 0.05$, **$p < 0.01$, ***$p < 0.001$.

4. Discussion

4.1. Analysis of extra- and intracellular concentrations of DINCH and MINCH

Considering that adipose tissue is an important endocrine organ through the secretion of adipokines (Kershaw and Flier, 2004; Trayhurn, 2014), e.g. leptin, mediating satiety and hunger, there is growing evidence that adipose tissue is sensitive to perturbations by MDCs (Biemann et al., 2021; Janesick and Blumberg, 2016). Following the restriction of the potential obesogen DEHP (European Parliament and the Council of the European Union, 2005; United States Congress, 2008), there has been a shift to substitution products such as the emerging plasticizer DINCH. However, similar to the DEHP metabolite MEHP, the primary metabolite MINCH induced adipocyte differentiation in rat and human adipocytes, although in the μM concentration range (Campioli et al., 2015; Schaffert et al., 2022). Consistent with these results, we were able to confirm that MINCH in the μM concentration range, but not DINCH, induced lipid accumulation in human SGBS cells (Supplementary Figure 4).

To further investigate which actual concentrations cause the phenotypical effects and whether these effects are reflected by internal uptake of the tested chemical, we measured the concentrations of DINCH and MINCH in our cell culture model. Analysis of the conditioned medium with the chemicals before cell incubation revealed that the solubility of DINCH was limited, unlike MINCH. The nominal concentration of 10 μM contained only 500 nM DINCH (Fig. 1A). Thus, it is possible that the lack of phenotypical effects by DINCH treatment observed in this study, as well as in previous *in vitro* studies, is due to the failure to obtain sufficiently high concentrations to induce a cellular response. Nevertheless, in the case of DEHP, which has a log K_{ow} two orders of magnitude lower than DINCH (DEHP log K_{ow} exp. 7.5 (Bruijn et al., 1989); DINCH log K_{ow} est. 9.8; MINCH log K_{ow} est. 5.2 (McNally et al., 2019)) and thus a much higher water-solubility, only the metabolite MEHP induces adipogenesis, not the parent compound (Feige et al., 2007). Consistent with this observation, no binding to PPARG and activation was observed for both DEHP and DINCH, in contrast to MEHP and MINCH (Kratochvil et al., 2019; Schaffert et al., 2022).

Measurement of DINCH and MINCH in conditioned medium after 48 h treatment of SGBS cells indicated intracellular uptake of the chemicals, due to a 2- to 5-fold dose reduction. Several interdependent factors including absorption to the plastic walls of the cell culture plates or soluble proteins, degradation of the chemical, but also intracellular uptake can lead to this dose reduction (Dimitrijevic et al., 2022). By analyzing concentrations of DINCH and MINCH in the cell lysates after 12 days, we confirmed the cellular uptake of both DINCH and MINCH (Fig. 1B). This uptake was concentration-dependent in a linear manner and was observed even in cells treated with 10 nM of DINCH, where detection in the cell culture medium before incubation was below the LOD (<5.5 nM). We thus speculate that DINCH, due to its hydrophobic nature, is dispersed in the cell culture medium and, even if present in very low amounts, is readily adsorbed by the hydrophobic parts of the adipocyte cell, such as lipids or the lipid membrane, where it can accumulate over time. *In vivo*, however, current toxicokinetic data from Wistar rats do not indicate bioaccumulation of DINCH in adipose tissue, as it is rapidly eliminated (Langsch et al., 2018).

We further characterized the effects of DINCH exposure in our *in vitro* system by analyzing possible biotransformation, which has to our information not been considered in other *in vitro* studies testing DINCH before. In SGSB cells treated with 10 μM DINCH (nominal concentration), 5 nM MINCH was detected in medium supernatant after 48 h (Fig. 2). In contrast, no conversion of DINCH to MINCH was observed under abiotic conditions confirming that the transformation is dependent on the presence of cells (Fig. 2). Similar to DINCH, the metabolization of DEHP to MEHP was characterized previously (Schaedlich et al., 2018), matching the transformation rate of DINCH observed here.

We suggest that the extracellular phase I biotransformation of DINCH is mainly due to the cell-surface associated lipoprotein lipase which is a known factor for the hydrolysis of phthalates and characteristically expressed in SGBS cells (Gonzales and Orlando, 2007; Harris et al., 2016; Wabitsch et al., 2001). The presence of the highly abundant lipases ATGL, HSL, and MGL in SGBS cells necessary for lipolysis provides additional intracellular biotransformation capacity (Kalkhof et al., 2020).

Analysis of intracellular concentrations revealed that after 12 days of treatment with 10 μM DINCH, MINCH is detected at a similar concentration level to SGBS cells treated with approximately 37 nM MINCH for

12 days (Fig. 2). This concentration range explains the absence of MINCH-induced effects in DINCH-treated SGBS cells as no phenotypical changes were observed by the 10 nM and 100 nM MINCH treatment.

Further biotransformation of MINCH into the secondary metabolites oxo-MINCH, OH-MINCH, and cx-MINCH could not be detected in SGBS cells treated with 10 μM of the DINCH-conditioned medium. We hypothesize that this is due to the limited solubility of DINCH and the slow conversion rate of DINCH to MINCH (1:100 of the original dose after 48 h). However, in SGBS cells treated with 10 μM of the conditioned MINCH medium, we observed low concentrations of OH-MINCH in the supernatant after 48 h and intracellularly at day 12, which is consistent with the fact that SGBS cells express cytochrome P450 family enzymes capable of performing these oxidation reactions (Kalkhof et al., 2020; Li et al., 2014). Nevertheless, the further biotransformation capacity of SGBS cells is limited, as the conversion rate (1:6000 of the original dose after 48 h) is an order of magnitude lower than the conversion of DINCH to MINCH. This is consistent with the observations of Schaedlich et al. who observed only minimal conversion of DEHP to the oxidized DEHP metabolites (Schaedlich et al., 2018).

Our results highlight the importance of determining the absolute concentrations and the analysis of the biotransformation process for studying new chemicals by *in vitro* toxicology assays (Fischer et al., 2018).

4.2. Effects of MINCH and DINCH on adipocyte metabolism

After confirming that the phenotypic changes were in accordance with the intracellular uptake of the plasticizers, we investigated the effects of DINCH and MINCH on the central carbon metabolism in adipocytes, since our previous study indicated a strong effect on the cellular metabolism on proteome level (Schaffert et al., 2022) without deciphering the affected metabolites.

Comparison of SGBS cells differentiated with rosiglitazone to the untreated control revealed a strong increase in metabolite levels in the core metabolic pathways glycolysis, PPP, and parts of the TCA cycle (fumarate to oxaloacetate; Fig. 3B). The observed increase in metabolite levels indicates a higher metabolic activity, i.e. flux through these pathways. This is consistent with the observations of Roberts et al. and Oates and Antoniewicz, who analyzed the differentiation process of 3T3-L1 cells and found an upregulation of metabolite levels (Roberts et al., 2009) as well as an increased flux through glycolysis, PPP, and the TCA in differentiated adipocytes (Oates and Antoniewicz, 2022). Similar to rosiglitazone, we observed increased metabolite levels of lower glycolysis, lactate, acetyl-CoA, and oxaloacetate in cells treated with 10 μM MINCH (Fig. 3B).

Thus, we partially observed a similar metabolic response of MINCH at a concentration of 10 μM compared to rosiglitazone. In contrast, neither the lower concentrations of MINCH nor DINCH were able to induce significant metabolic changes compared to control cells. Since metabolite levels of glycolysis, PPP, and TCA are strongly altered during differentiation, reflecting altered pathway usage and increased flux (Oates and Antoniewicz, 2022; Roberts et al., 2009), this lack of metabolic response is probably due to the inability to induce adipogenesis of human SGBS cells (Supplementary Figure 4). In addition, the lower concentrations of MINCH and DINCH showed a higher variance in the measured metabolite levels of the central carbon metabolism (Fig. 3A). Although these treatments lack PPARG-agonistic activities that are crucial for complete differentiation, other additives to induce differentiation such as dexamethasone and IBMX are present, which alone induce minimal differentiation of the SGBS cells as previously described (Schaffert et al., 2022). Thus, the higher variance observed probably reflects that the cells were in an intermediate state, i.e. neither fully preadipocyte nor mature adipocyte.

Interestingly, the most significant metabolic change in glycolysis observed in cells treated with 10 μM MINCH and rosiglitazone-differentiated cells was the increase in Gro3P levels (Fig. 3B). Gro3P plays an important role in adipocytes in the synthesis of triglycerides from fatty acids and the re-esterification of non-esterified fatty acids (Beale et al., 2003). It has been shown that the insulin-sensitizing effect of thiazolidinediones (TZDs) such as rosiglitazone occurs through activation of a futile cycle of triglyceride hydrolysis and re-synthesis involving increased production of Gro3P by glycolysis or glyceroneogenesis (Guan et al., 2002; Tordjman et al., 2003). Remarkably, the upregulation of glyceroneogenesis in primary human adipocytes by MEHP has been described and associated partly with its potential obesogenic effects, similar to the weight gain induced by TZD treatment (Ellero-Simatos et al., 2011). Elevated levels of the precursors for glyceroneogenesis, pyruvate, lactate, and alanine, observed in this study and the recently reported upregulation of the gluconeogenesis pathway by treatment with 10 μM MINCH (Schaffert et al., 2022), indicate that MINCH induces glyceroneogenesis in SGBS cells similar to rosiglitazone. Thus, MINCH might act similarly to MEHP on adipocyte metabolism.

Downstream of glycolysis, the observed difference in TCA cycle response by the rosiglitazone and the 10 μM MINCH treatment (Fig. 3B) is similar to the observation by Krycer et al. in 3T3-L1 metabolism after insulin stimulation. The increased metabolite levels of fumarate and malate were accounted to pyruvate anaplerosis by pyruvate carboxylase (PC) (Krycer et al., 2017). Indeed, the elevated levels of fumarate to oxaloacetate in rosiglitazone-differentiated cells and oxaloacetate in MINCH-treated cells treatment are indicative of the anaplerotic flux of pyruvate into the TCA cycle. This was confirmed by the strongly induced enzyme levels of PC reported for MINCH-treated and rosiglitazone-differentiated cells (Supplementary Figure 5) (Schaffert et al., 2022). Several metabolome studies using 3T3-L1 adipocytes have shown that pyruvate anaplerosis by PC is important for fatty acid biosynthesis and a hallmark of adipocyte differentiation (Krycer et al., 2017; Liu et al., 2016; Oates and Antoniewicz, 2022; Si et al., 2009).

In addition to PC, induction of ACLY, PDH, and CS was observed (Supplementary Figure 5). Together with increased acetyl-CoA and pyruvate levels, this suggests upregulation of the pyruvate cycle, which is relevant for the concerted production of NAPDH and generation of the fatty acid precursors acetyl-CoA (Liu et al., 2016; Oates and Antoniewicz, 2022). Thus, the interplay between the supply of acetyl-CoA and anaplerotic replenishment of the TCA cycle is an important driver of *de novo* lipogenesis induced by MINCH and rosiglitazone in SGBS cells.

4.3. Insulin response of DINCH- and MINCH-treated SGBS preadipocytes

In contrast to the similarities in central carbon metabolism observed between rosiglitazone and MINCH, we found differences in the secretion of lactate. Cells treated with 10 μM MINCH had 19% higher lactate secretion than cells treated with rosiglitazone (Fig. 4). Lactate production is an important metabolic feature of adipocytes (Krycer et al., 2020) and adipose tissue is known to be a major producer of lactate (DiGirolamo et al., 1992). Analysis of lactate production by human adipose tissue has shown that up to 60%–80% of metabolized glucose is converted to lactate (Mårin et al., 1987). Importantly, increased lactate adipocyte production by adipose tissue and elevated plasma lactate concentrations in humans are associated with obesity and insulin resistance (Chen et al., 1993; DiGirolamo et al., 1992; Lin et al., 2022).

We thus tested the short-term metabolic insulin response of MINCH-treated cells and compared it to rosiglitazone-differentiated cells. Overall, the insulin response of glycolysis and PPP was similar between MINCH-treated and rosiglitazone-differentiated cells (Fig. 5). Differences were observed for PEP and acetyl-CoA, which showed decreased and increased fold-change by MINCH treatment, respectively. This suggests that MINCH-treated cells divert higher PEP levels towards acetyl-CoA upon insulin stimulation.

In conclusion, we did not observe differences in the insulin response of MINCH-treated SGBS adipocytes to rosiglitazone-differentiated adipocytes, indicating that MINCH treatment does not induce insulin resistance. Nevertheless, future work should investigate whether known

adipogenic chemicals could lead to higher lactate secretion in adipocytes as well as in adipose tissue *in vivo* or explants *ex vivo*. Since adipocyte-derived lactate has recently been shown to act as a signaling molecule that promotes macrophage inflammation and thereby induces insulin resistance in mice and humans (Feng et al., 2022), this may contribute to the understanding of whether MDCs induce adipose tissue inflammation and insulin resistance *via* this mechanism.

4.4. PPARG-dependent and -independent effects of DINCH and MINCH

Earlier studies have shown that MINCH is the bioactive metabolite promoting adipogenesis *via* binding and activation of the nuclear hormone receptor PPARG (Campioli et al., 2015; Schaffert et al., 2022). Furthermore, co-crystallization of human PPARG with MINCH recently confirmed that MINCH binds similarly to MEHP to the AF-2 site of the ligand binding pocket and thereby stabilizes it in an active conformation required for co-activator interaction (Useini et al., 2023). However, Campioli et al. suspected that PPARA and not PPARG is the main initiator of MINCH effects, based on their observation that the adipogenesis-inducing effect of MINCH was blocked by a PPARA antagonist and only partially by a PPARG antagonist.

We investigated the effects induced by MINCH in the presence of 10 μM of the selective PPARG inhibitor GW9662. Lipid accumulation and metabolic effects by MINCH were markedly reduced under PPARG inhibition (Fig. 6), suggesting that the adipogenesis-inducing effect of MINCH is mainly PPARG-dependent. Nevertheless, lipid accumulation was still significantly higher in cells treated with MINCH and the inhibitor than in cells treated with the inhibitor alone (Fig. 6A, Supplementary Figure 9). At the metabolic level, the significantly elevated acetyl-CoA and oxaloacetate levels upon MINCH treatment in the presence of the inhibitor were indicative of an upregulated pyruvate cycle as in treatment without inhibitor (Fig. 6B). Similarly, lactate secretion was significantly upregulated by MINCH treatment in the presence of the inhibitor (Fig. 6B). Taken together, this suggests that MINCH exerts its effects on adipocyte metabolism at least to a small part *via* a PPARG-independent mechanism such as *via* PPARA. In 3T3-L1 adipocytes, activation of PPARA induced adipogenesis in the absence of lipid accumulation, similar to what was observed here (Goto et al., 2011). In addition, it was recently reported that activation of PPARG target genes alongside activation of PPARA target genes was induced by MINCH treatment in SGBS cells (Schaffert et al., 2022). Furthermore, Engel et al. observed a concentration-dependent induction of PPARA activity in a GAL4-UAS reporter gene assay (Engel et al., 2018). Because PPARG and PPARA share structural similarities and overlapping transcriptional activities (Tachibana et al., 2005; Xu et al., 2001), further studies are needed to dissect the precise role of PPARA in the adipogenesis-inducing effect of MINCH and to determine whether other nuclear receptors might play additional roles.

Similar to MINCH treatment in the presence of the inhibitor, we observed significantly higher lipid content in cells treated with rosiglitazone and GW9662 compared to cells treated with the inhibitor alone (Fig. 6A, Supplementary Figure 9). This is unexpected since rosiglitazone is mainly described as a selective PPARG agonist. We ensured irreversible PPARG inhibition by using a concentration of 10 μM and adding GW9662 regularly every other day before treatment. Thus, our observation suggests a possible PPARG-independent mechanism of lipid induction by rosiglitazone. Although PPARG-independent effects of rosiglitazone have already been described on breast tumor cells in the context of tumor growth (Seargent et al., 2004) and on renal tubules in the context of glucose metabolism (Derlacz et al., 2008), to our knowledge PPARG-independent effects of rosiglitazone on adipocytes are lacking, indicating the need for further investigation of this hypothesis.

An important question for assessing the safety of chemicals by *in vitro* toxicology is whether the observed effects of the tested chemical occur at environmentally relevant concentrations. Due to the steadily increasing use of DINCH, several biomonitoring studies show an increase in urinary concentrations of DINCH metabolites, especially in the EU and the USA (Gyllenhammar et al., 2017; Schütze et al., 2014; Silva et al., 2013). Recent exposure data from the HBM4EU project show that the geometric mean value of DINCH metabolites in the urine of children in Europe is 3.57 μg/L and of adolescents in Europe 2.51 μg/L (Vogel et al., 2023). These concentrations are three orders of magnitude lower than the MINCH concentration at which adipogenesis-promoting effects were observed in our study. While urine biomonitoring is well established, concentrations of DINCH and its metabolites in human serum that even better approximate the concentrations expected in adipose tissue are lacking to date. Studies that analyzed serum concentrations of DEHP metabolites in adult men and women showed that they are detected in the low nM range (2–10 nM) (Högberg et al., 2008; Specht et al., 2014). In our study, we did not observe any effects of MINCH in this low concentration range, but only in the low μM range, which is unlikely to be reached in the general population *in vivo*.

Thus, the high doses of MINCH may be only relevant under specific exposure conditions. As DINCH is used as a substitute for DEHP in medical devices, medical treatment may result in much higher exposure than that of the general population (Šimunović et al., 2022). In ICU patients, exposure to DEHP was ~100-1000-fold higher compared to the general adult population, with DEHP metabolites reaching serum levels of >10 μM (Huygh et al., 2015). However, since these are only human serum values for DEHP metabolites and a lower migration of DINCH compared to DEHP from blood bags was observed (Zhong et al., 2013), this underlines the need to analyze the concentrations of DINCH and its metabolites in human serum (general population and intensive care patients). In addition, experimental validation and determination of other data relevant to the determination of bioavailability is required, such as the proportion of protein-bound MINCH, which is currently only estimated (McNally et al., 2019). Taken together, these values could further improve the currently developed pharmacokinetic models for DINCH (Espié et al., 2009; McNally et al., 2019) and lead to a more accurate estimate of the absolute concentrations of DINCH and its metabolites in human adipose tissue.

In addition to determining serum levels, further studies are needed to assess whether MINCH may contribute to the effects of chemical mixtures and whether synergistic effects of plasticizer mixtures containing MINCH could lead to a potential obesogenic effect *in vivo* (Carpenter et al., 2002; Ghisari and Bonefeld-Jorgensen, 2009).

Overall, no adipogenic capacity of MINCH was observed in human SGBS cells at environmentally relevant concentrations. This is consistent with the results of previous *in vivo* studies, including a two-generation study, repeated-dose toxicity studies, and a combined chronic and carcinogenic study in Wistar rats, in which no weight-promoting effects were observed (Harmon and Otter, 2022; Langsch et al., 2018). Similarly, no increased fat pad weight or total weight was observed after *in utero* DINCH exposure of Sprague-Dawley rats at postnatal day 60 and 200 (Campioli et al., 2017). In the absence of specific test methods for metabolic disruption and in light of the 3R principles for animal testing, our method could therefore serve as NAM (Braeuning et al., 2023; Schmeisser et al., 2023) for the assessment of adipogenic effects.

5. Conclusion

By combining *in vitro* concentration analysis and targeted metabolomics of human SGBS cells exposed to DINCH and MINCH, our study provides insights into how analysis of the core metabolism of human adipocytes could serve as a method for assessing the potential adipogenic capacity of chemicals. Treatment of human SGBS adipocytes revealed a linearly dependent cellular uptake of DINCH and MINCH, as well as biotransformation of DINCH to MINCH and MINCH to OH-MINCH (Fig. 7). Intracellular uptake of MINCH, but not DINCH, was associated with metabolic rewiring in central carbon metabolism towards lipid accumulation and induction of adipogenesis primarily through upregulation of the pyruvate cycle (Fig. 7).

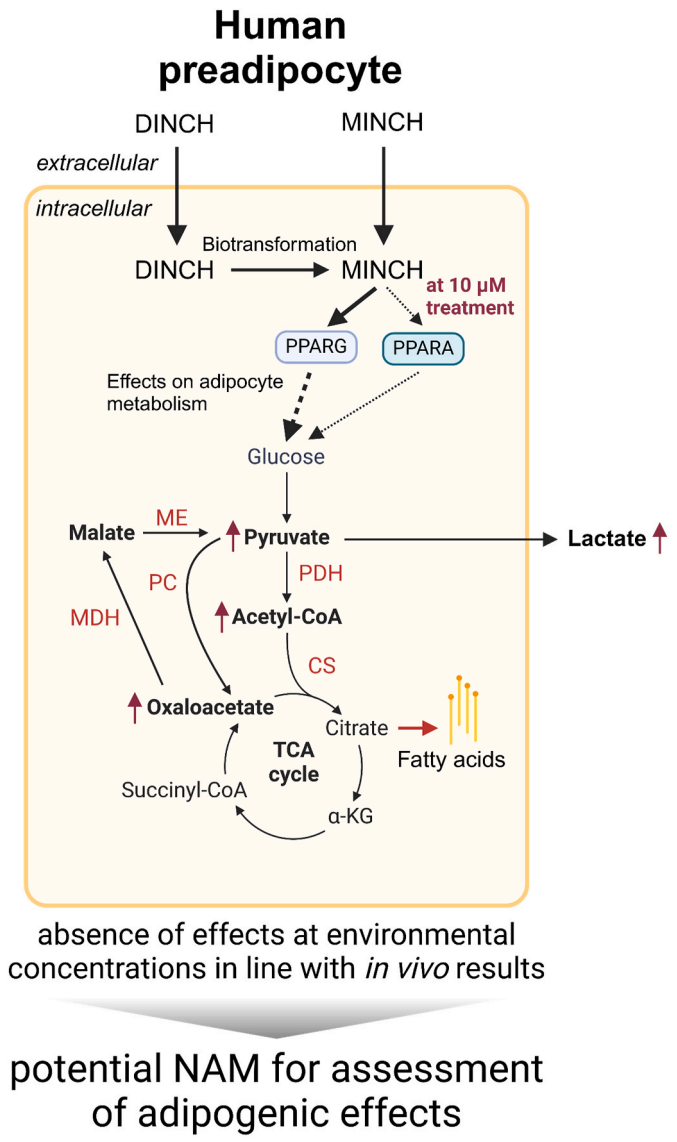

Fig. 7. Analysis of the effects of DINCH and MINCH on human adipocyte metabolism. Cellular uptake of DINCH and MINCH, as well as biotransformation of DINCH to MINCH, was validated in SGBS preadipocytes. After cellular uptake, MINCH leads to upregulation of the pyruvate cycle *via* PPARG-dependent and independent mechanism thereby shifting metabolism towards adipogenesis and lipid accumulation. In addition, elevated lactate secretion was induced by MINCH treatment. However, the effects of MINCH were only observed in the µM concentration range, which is three times higher than the concentration of other phthalate plasticizers found in human serum. The absence of effects at more physiologically relevant concentrations is thus consistent with the results of previous *in vivo* studies and emphasizes that our method may be a potential NAM for the assessment of adipogenic effects. CS – citrate synthase, MDH – malate dehydrogenase, ME – malic enzyme, PC – pyruvate carboxylase, PDH – pyruvate dehydrogenase (red arrows – elevated metabolite level; red marked protein name – elevated enzyme level).

However, the changes upon treatment with MINCH were only observed in the µM concentration range, which is three orders of magnitude higher than concentrations of phthalate plasticizers found in human serum. More physiologically relevant MINCH concentrations in the low nM range showed no adipogenesis-promoting effects, which is consistent with current *in vivo* results. Nevertheless, further research is needed to analyze whether MINCH could contribute to the cumulative effects of chemical mixtures. Considering the lack of tests to identify metabolism-disrupting effects of chemicals, this highlights that our method could be used as a NAM for the assessment of potential adipogenic properties of chemicals and help to avoid animal studies.

Funding

This research was funded by the German Research Foundation (Deutsche Forschungsgemeinschaft, DFG) through the CRC 1052 "Obesity Mechanisms", project number 209933838 (B1 MB, C7 JTH, Z3 MvB). Furthermore, this work was carried out in the framework of the European Partnership for the Assessment of Risks from Chemicals (PARC) - P5.2.1.b MD-ED - and has received funding from the European Union's Horizon Europe research and innovation programme under Grant Agreement No. 101057014. Views and opinions expressed are however those of the author(s) only and do not necessarily reflect those of the European Union or the Health and Digital Executive Agency. Neither the European Union nor the granting authority can be held responsible for them. K.S. is grateful for funding by the German Research Foundation (project no. 530364326).

CRediT authorship contribution statement

Cornelius Goerdeler: Writing – original draft, Visualization, Validation, Methodology, Formal analysis, Data curation, Conceptualization. **Beatrice Engelmann:** Writing – review & editing, Validation, Supervision, Methodology, Conceptualization. **Alix Sarah Aldehoff:** Writing – review & editing, Formal analysis. **Alexandra Schaffert:** Writing – review & editing, Conceptualization. **Matthias Blüher:** Writing – review & editing, Project administration, Funding acquisition. **John T. Heiker:** Writing – review & editing. **Martin Wabitsch:** Writing – review & editing, Resources. **Kristin Schubert:** Writing – review & editing. **Ulrike Rolle-Kampczyk:** Writing – review & editing, Supervision, Conceptualization. **Martin von Bergen:** Writing – review & editing, Resources, Funding acquisition.

Declaration of competing interest

The authors declare that they have no known competing financial interests or personal relationships that could have appeared to influence the work reported in this paper.

Data availability

The metabolome data of all three studies are available at the NIH Common Fund's National Metabolomics Data Repository (NMDR) website, the Metabolomics Workbench, where it has been assigned the project ID PR001814. The data can be accessed directly *via* https://doi.org/10.21228/M87D9M.

Acknowledgment

We thank Olivia Pleβow and Nicole Bock for technical assistance with the LC-MS measurements. We are grateful for the support of the NMDR/Metabolomics Workbench which is supported by NIH grant U2C-DK119886 and OT2-OD030544 grants. The graphical abstract, Figs. 4, 5 and 7, and Supplementary Figure 3 were created using BioRender.com.

Appendix ASupplementary data

Supplementary data to this article can be found online at https://doi.org/10.1016/j.envres.2024.118847.

References

Axelsson, J., Rylander, L., Rignell-Hydbom, A., Jönsson, B.A.G., Lindh, C.H., Giwercman, A., 2015. Phthalate exposure and reproductive parameters in young

men from the general Swedish population. Environ. Int. 85, 54–60. https://doi.org/10.1016/j.envint.2015.07.005.
Beale, E.G., Antoine, B., Forest, C., 2003. Glyceroneogenesis in adipocytes: another textbook case. Trends Biochem. Sci. 28, 402–403. https://doi.org/10.1016/S0968-0004(03)00163-4.
Bell, C.G., Walley, A.J., Froguel, P., 2005. The genetics of human obesity. Nat. Rev. Genet. 6, 221–234. https://doi.org/10.1038/nrg1556.
Biemann, R., Blüher, M., Isermann, B., 2021. Exposure to endocrine-disrupting compounds such as phthalates and bisphenol A is associated with an increased risk for obesity. Best Pract. Res. Cl. En. 35, 101546 https://doi.org/10.1016/j.beem.2021.101546.
Biemann, R., Navarrete Santos, A., Navarrete Santos, A., Riemann, D., Knelangen, J., Blüher, M., Koch, H., Fischer, B., 2012. Endocrine disrupting chemicals affect the adipogenic differentiation of mesenchymal stem cells in distinct ontogenetic windows. Biochem. Bioph. Res. Co. 417, 747–752. https://doi.org/10.1016/j.bbrc.2011.12.028.
Blüher, M., 2019. Obesity: global epidemiology and pathogenesis. Nat. Rev. Endocrinol. 15, 288–298. https://doi.org/10.1038/s41574-019-0176-8.
Braeuning, A., Balaguer, P., Bourguet, W., Carreras-Puigvert, J., Feiertag, K., Kamstra, J. H., Knapen, D., Lichtenstein, D., Marx-Stoelting, P., Rietdijk, J., Schubert, K., Spjuth, O., Stinckens, E., Thedieck, K., van den Boom, R., Vergauwen, L., Bergen, M. von, Wewer, N., Zalko, D., 2023. Development of new approach methods for the identification and characterization of endocrine metabolic disruptors-a PARC project. Front. Toxicol. 5, 1212509 https://doi.org/10.3389/ftox.2023.1212509.
Bruijn, J. de, Busser, F., Seinen, W., Hermens, J., 1989. Determination of octanol/water partition coefficients for hydrophobic organic chemicals with the "slow-stirring" method. Environ. Toxicol. Chem. 8, 499–512. https://doi.org/10.1002/etc.5620080607.
Buescher, J.M., Moco, S., Sauer, U., Zamboni, N., 2010. Ultrahigh performance liquid chromatography-tandem mass spectrometry method for fast and robust quantification of anionic and aromatic metabolites. Anal. Chem. 82, 4403–4412. https://doi.org/10.1021/ac100101d.
Campioli, E., Duong, T.B., Deschamps, F., Papadopoulos, V., 2015. Cyclohexane-1,2-dicarboxylic acid diisononyl ester and metabolite effects on rat epididymal stromal vascular fraction differentiation of adipose tissue. Environ. Res. 140, 145–156. https://doi.org/10.1016/j.envres.2015.03.036.
Campioli, E., Lee, S., Lau, M., Marques, L., Papadopoulos, V., 2017. Effect of prenatal DINCH plasticizer exposure on rat offspring testicular function and metabolism. Sci. Rep. 7, 11072 https://doi.org/10.1038/s41598-017-11325-7.
Carpenter, D.O., Arcaro, K., Spink, D.C., 2002. Understanding the human health effects of chemical mixtures. Environ. Health Perspect. 110 (Suppl. 1), 25–42. https://doi.org/10.1289/ehp.02110s125.
Chen, Y.D., Varasteh, B.B., Reaven, G.M., 1993. Plasma lactate concentration in obesity and type 2 diabetes. Diabete Metab. 19, 348–354.
Darbre, P.D., 2017. Endocrine disruptors and obesity. Curr. Obes. Rep. 6, 18–27. https://doi.org/10.1007/s13679-017-0240-4.
Derlacz, R.A., Hyc, K., Usarek, M., Jagielski, A.K., Drozak, J., Jarzyna, R., 2008. PPAR-gamma-independent inhibitory effect of rosiglitazone on glucose synthesis in primary cultured rabbit kidney-cortex tubules. Biochem. Cell. Biol. 86, 396–404. https://doi.org/10.1139/o08-105.
Desdoits-Lethimonier, C., Albert, O., Le Bizec, B., Perdu, E., Zalko, D., Courant, F., Lesné, L., Guillé, F., Dejucq-Rainsford, N., Jégou, B., 2012. Human testis steroidogenesis is inhibited by phthalates. Hum. Reprod. 27, 1451–1459. https://doi.org/10.1093/humrep/des069.
DiGirolamo, M., Newby, F.D., Lovejoy, J., 1992. Lactate production in adipose tissue: a regulated function with extra-adipose implications. Faseb. J. 6, 2405–2412. https://doi.org/10.1096/fasebj.6.7.1563593.
Dimitrijevic, D., Fabian, E., Nicol, B., Funk-Weyer, D., Landsiedel, R., 2022. Toward realistic dosimetry in vitro: determining effective concentrations of test substances in cell culture and their prediction by an in silico mass balance model. Chem. Res. Toxicol. 35, 1962–1973. https://doi.org/10.1021/acs.chemrestox.2c00128.
Ellero-Simatos, S., Claus, S.P., Benelli, C., Forest, C., Letourneur, F., Cagnard, N., Beaune, P.H., Waziers, I. de, 2011. Combined transcriptomic-(1)H NMR metabonomic study reveals that monoethylhexyl phthalate stimulates adipogenesis and glyceroneogenesis in human adipocytes. J. Proteome Res. 10, 5493–5502. https://doi.org/10.1021/pr200765v.
Engel, A., Buhrke, T., Kasper, S., Behr, A.-C., Braeuning, A., Jessel, S., Seidel, A., Völkel, W., Lampen, A., 2018. The urinary metabolites of DINCH® have an impact on the activities of the human nuclear receptors ERα, ERβ, AR, PPARα and PPARγ. Toxicol. Lett. 287, 83–91. https://doi.org/10.1016/j.toxlet.2018.02.006.
Espié, P., Tytgat, D., Sargentini-Maier, M.-L., Poggesi, I., Watelet, J.-B., 2009. Physiologically based pharmacokinetics (PBPK). Drug Metab. Rev. 41, 391–407. https://doi.org/10.1080/10837450902891360.
EU Commission, 1999. 1999/815/EC: Commission Decision of 7 December 1999 adopting measures prohibiting the placing on the market of toys and childcare articles intended to be placed in the mouth by children under three years of age made of soft PVC containing one or more of the substances di-iso-nonyl phthalate (DINP), di(2-ethylhexyl) phthalate (DEHP). Dibutyl Phthalate (DBP), Di-iso-decyl Phthalate (DIDP), Di-n-octyl Phthalate (DNOP), and Butylbenzyl Phthalate (BBP).
European Parliament and the Council of the European Union, 2005. Directive 2005/84/EC of the European Parliament and of the Council Amending for the 22nd Time Council Directive 76/769/EEC on the Approximation of the Laws, Regulations and Administrative Provisions of the Member States Relating to Restrictions on the Marketing and Use of Certain Dangerous Substances and Preparations (Phthalates in Toys and Childcare Articles).
Feige, J.N., Gelman, L., Rossi, D., Zoete, V., Métivier, R., Tudor, C., Anghel, S.I., Grosdidier, A., Lathion, C., Engelborghs, Y., Michielin, O., Wahli, W., Desvergne, B., 2007. The endocrine disruptor monoethyl-hexyl-phthalate is a selective peroxisome proliferator-activated receptor gamma modulator that promotes adipogenesis. J. Biol. Chem. 282, 19152–19166. https://doi.org/10.1074/jbc.M702724200.
Feng, T., Zhao, X., Gu, P., Yang, W., Wang, C., Guo, Q., Long, Q., Liu, Q., Cheng, Y., Li, J., Cheung, C.K.Y., Wu, D., Kong, X., Xu, Y., Ye, D., Hua, S., Loomes, K., Xu, A., Hui, X., 2022. Adipocyte-derived lactate is a signalling metabolite that potentiates adipose macrophage inflammation via targeting PHD2. Nat. Commun. 13, 5208. https://doi.org/10.1038/s41467-022-32871-3.
Fischer, F.C., Abele, C., Droge, S.T.J., Henneberger, L., König, M., Schlichting, R., Scholz, S., Escher, B.I., 2018. Cellular uptake kinetics of neutral and charged chemicals in in vitro assays measured by fluorescence microscopy. Chem. Res. Toxicol. 31, 646–657. https://doi.org/10.1021/acs.chemrestox.8b00019.
Frederiksen, H., Jørgensen, N., Andersson, A.-M., 2010. Correlations between phthalate metabolites in urine, serum, and seminal plasma from young Danish men determined by isotope dilution liquid chromatography tandem mass spectrometry. J. Anal. Toxicol. 34, 400–410. https://doi.org/10.1093/jat/34.7.400.
Frohnert Hansen, J., Boas, M., Møller Brorson, M., Frederiksen, H., Hartoft-Nielsen, M.-L., Krogh Rasmussen, Å., Main, K.M., Feldt-Rasmussen, U., 2016. Migration of phthalates on culture plates - an important challenge to consider for in vitro studies. Scand. J. Clin. Lab. Invest. 76, 165–171. https://doi.org/10.3109/00365513.2015.1110857.
Gepstein, V., Weiss, R., 2019. Obesity as the main risk factor for metabolic syndrome in children. Front. Endocrinol. 10, 568. https://doi.org/10.3389/fendo.2019.00568.
Ghisari, M., Bonefeld-Jorgensen, E.C., 2009. Effects of plasticizers and their mixtures on estrogen receptor and thyroid hormone functions. Toxicol. Lett. 189, 67–77. https://doi.org/10.1016/j.toxlet.2009.05.004.
Gonzales, A.M., Orlando, R.A., 2007. Role of adipocyte-derived lipoprotein lipase in adipocyte hypertrophy. Nutr. Metab. 4, 22. https://doi.org/10.1186/1743-7075-4-22.
Goto, T., Lee, J.-Y., Teraminami, A., Kim, Y.-I., Hirai, S., Uemura, T., Inoue, H., Takahashi, N., Kawada, T., 2011. Activation of peroxisome proliferator-activated receptor-alpha stimulates both differentiation and fatty acid oxidation in adipocytes. J. Lipid Res. 52, 873–884. https://doi.org/10.1194/jlr.M011320.
Guan, H.-P., Li, Y., Jensen, M.V., Newgard, C.B., Steppan, C.M., Lazar, M.A., 2002. A futile metabolic cycle activated in adipocytes by antidiabetic agents. Nat. Med. 8, 1122–1128. https://doi.org/10.1038/nm780.
Guh, D.P., Zhang, W., Bansback, N., Amarsi, Z., Birmingham, C.L., Anis, A.H., 2009. The incidence of co-morbidities related to obesity and overweight: a systematic review and meta-analysis. BMC Publ. Health 9, 88. https://doi.org/10.1186/1471-2458-9-88.
Gyllenhammar, I., Glynn, A., Jönsson, B.A.G., Lindh, C.H., Darnerud, P.O., Svensson, K., Lignell, S., 2017. Diverging temporal trends of human exposure to bisphenols and plastizisers, such as phthalates, caused by substitution of legacy EDCs? Environ. Res. 153, 48–54. https://doi.org/10.1016/j.envres.2016.11.012.
Hall, K.D., Ayuketah, A., Brychta, R., Cai, H., Cassimatis, T., Chen, K.Y., Chung, S.T., Costa, E., Courville, A., Darcey, V., Fletcher, L.A., Forde, C.G., Gharib, A.M., Guo, J., Howard, R., Joseph, P.V., McGehee, S., Ouwerkerk, R., Raisinger, K., Rozga, I., Stagliano, M., Walter, M., Walter, P.J., Yang, S., Zhou, M., 2019. Ultra-processed diets cause excess calorie intake and weight gain: an inpatient randomized controlled trial of ad libitum food intake. Cell Metabol. 30, 67–77.e3. https://doi.org/10.1016/j.cmet.2019.05.008.
Hansen, J.F., Nielsen, C.H., Brorson, M.M., Frederiksen, H., Hartoft-Nielsen, M.-L., Rasmussen, Å.K., Bendtzen, K., Feldt-Rasmussen, U., 2015. Influence of phthalates on in vitro innate and adaptive immune responses. PLoS One 10, e0131168. https://doi.org/10.1371/journal.pone.0131168.
Hao, C., Cheng, X., Xia, H., Ma, X., 2012. The endocrine disruptor mono-(2-ethylhexyl) phthalate promotes adipocyte differentiation and induces obesity in mice. Biosci. Rep. 32, 619–629. https://doi.org/10.1042/BSR20120042.
Harmon, P., Otter, R., 2022. A review of common non-ortho-phthalate plasticizers for use in food contact materials. Food Chem. Toxicol. 164, 112984 https://doi.org/10.1016/j.fct.2022.112984.
Harris, S., Wegner, S., Hong, S.W., Faustman, E.M., 2016. Phthalate metabolism and kinetics in an in vitro model of testis development. Toxicol. Vitro 32, 123–131. https://doi.org/10.1016/j.tiv.2015.12.002.
Heindel, J.J., Blumberg, B., Cave, M., Machtinger, R., Mantovani, A., Mendez, M.A., Nadal, A., Palanza, P., Panzica, G., Sargis, R., Vandenberg, L.N., vom Saal, F., 2017. Metabolism disrupting chemicals and metabolic disorders. Reprod. Toxicol. 68, 3–33. https://doi.org/10.1016/j.reprotox.2016.10.001.
Hennebert, P., 2022. Hazardous properties of plasticisers that may hinder the recycling of plastics. Detritus 35–44. https://doi.org/10.31025/2611-4135/2022.17227.
Högberg, J., Hanberg, A., Berglund, M., Skerfving, S., Remberger, M., Calafat, A.M., Filipsson, A.F., Jansson, B., Johansson, N., Appelgren, M., Håkansson, H., 2008. Phthalate diesters and their metabolites in human breast milk, blood or serum, and urine as biomarkers of exposure in vulnerable populations. Environ. Health Perspect. 116, 334–339. https://doi.org/10.1289/ehp.10788.
Hurst, C.H., Waxman, D.J., 2003. Activation of PPARalpha and PPARgamma by environmental phthalate monoesters. Toxicol. Sci. 74, 297–308. https://doi.org/10.1093/toxsci/kfg145.
Huygh, J., Clotman, K., Malarvannan, G., Covaci, A., Schepens, T., Verbrugghe, W., Dirinck, E., van Gaal, L., Jorens, P.G., 2015. Considerable exposure to the endocrine disrupting chemicals phthalates and bisphenol-A in intensive care unit (ICU) patients. Environ. Int. 81, 64–72. https://doi.org/10.1016/j.envint.2015.04.008.
Janesick, A.S., Blumberg, B., 2016. Obesogens: an emerging threat to public health. Am. J. Obstet. Gynecol. 214, 559–565. https://doi.org/10.1016/j.ajog.2016.01.182.

Kalkhof, S., Krieg, L., Büttner, P., Wabitsch, M., Küntzel, C., Friebe, D., Landgraf, K., Hanschkow, M., Schubert, K., Kiess, W., Krohn, K., Blüher, M., Bergen, M. von, Körner, A., 2020. In depth quantitative proteomic and transcriptomic characterization of human adipocyte differentiation using the SGBS cell line. Proteomics e1900405. https://doi.org/10.1002/pmic.201900405.

Kershaw, E.E., Flier, J.S., 2004. Adipose tissue as an endocrine organ. J. Clin. Endocrinol. Metab. 89, 2548–2556. https://doi.org/10.1210/jc.2004-0395.

Kim, J.H., Park, H., Lee, J., Cho, G., Choi, S., Choi, G., Kim, S.Y., Eun, S.-H., Suh, E., Kim, S.K., Kim, H.-J., Kim, G.-H., Lee, J.J., Kim, Y.D., Eom, S., Kim, S., Moon, H.-B., Park, J., Choi, K., Kim, S., Kim, S., 2016. Association of diethylhexyl phthalate with obesity-related markers and body mass change from birth to 3 months of age. J. Epidemiol. Community Health 70, 466–472. https://doi.org/10.1136/jech-2015-206315.

Klöting, N., Hesselbarth, N., Gericke, M., Kunath, A., Biemann, R., Chakaroun, R., Kosacka, J., Kovacs, P., Kern, M., Stumvoll, M., Fischer, B., Rolle-Kampczyk, U., Feltens, R., Otto, W., Wissenbach, D.K., Bergen, M. von, Blüher, M., 2015. Di-(2-Ethylhexyl)-Phthalate (DEHP) causes impaired adipocyte function and alters serum metabolites. PLoS One 10, e0143190. https://doi.org/10.1371/journal.pone.0143190.

Koch, H.M., Schütze, A., Pälmke, C., Angerer, J., Brüning, T., 2013. Metabolism of the plasticizer and phthalate substitute diisononyl-cyclohexane-1,2-dicarboxylate (DINCH(®)) in humans after single oral doses. Arch. Toxicol. 87, 799–806. https://doi.org/10.1007/s00204-012-0990-4.

Kratochvil, I., Hofmann, T., Rother, S., Schlichting, R., Moretti, R., Scharnweber, D., Hintze, V., Escher, B.I., Meiler, J., Kalkhof, S., Bergen, M. von, 2019. Mono(2-ethylhexyl) phthalate (MEHP) and mono(2-ethyl-5-oxohexyl) phthalate (MEOHP) but not di(2-ethylhexyl) phthalate (DEHP) bind productively to the peroxisome proliferator-activated receptor γ. Rapid Commun. Mass Spectrom. 33 (Suppl. 1), 75–85. https://doi.org/10.1002/rcm.8258.

Krycer, J.R., Quek, L.-E., Francis, D., Fazakerley, D.J., Elkington, S.D., Diaz-Vegas, A., Cooke, K.C., Weiss, F.C., Duan, X., Kurdyukov, S., Zhou, P.-X., Tambar, U.K., Hirayama, A., Ikeda, S., Kamei, Y., Soga, T., Cooney, G.J., James, D.E., 2020. Lactate production is a prioritized feature of adipocyte metabolism. J. Biol. Chem. 295, 83–98. https://doi.org/10.1074/jbc.RA119.011178.

Krycer, J.R., Yugi, K., Hirayama, A., Fazakerley, D.J., Quek, L.-E., Scalzo, R., Ohno, S., Hodson, M.P., Ikeda, S., Shoji, F., Suzuki, K., Domanova, W., Parker, B.L., Nelson, M. E., Humphrey, S.J., Turner, N., Hoehn, K.L., Cooney, G.J., Soga, T., Kuroda, S., James, D.E., 2017. Dynamic metabolomics reveals that insulin primes the adipocyte for glucose metabolism. Cell Rep. 21, 3536–3547. https://doi.org/10.1016/j.celrep.2017.11.085.

Langsch, A., David, R.M., Schneider, S., Sperber, S., Haake, V., Kamp, H., Leibold, E., van Ravenzwaay, B., Otter, R., 2018. Hexamoll® DINCH: lack of in vivo evidence for obesogenic properties. Toxicol. Lett. 288, 99–110. https://doi.org/10.1016/j.toxlet.2018.02.008.

Li, J., Daly, E., Campioli, E., Wabitsch, M., Papadopoulos, V., 2014. De novo synthesis of steroids and oxysterols in adipocytes. J. Biol. Chem. 289, 747–764. https://doi.org/10.1074/jbc.M113.534172.

Li, X., Ycaza, J., Blumberg, B., 2011. The environmental obesogen tributyltin chloride acts via peroxisome proliferator activated receptor gamma to induce adipogenesis in murine 3T3-L1 preadipocytes. J. Steroid Biochem. Mol. Biol. 127, 9–15. https://doi.org/10.1016/j.jsbmb.2011.03.012.

Lin, Y., Bai, M., Wang, S., Chen, L., Li, Z., Li, C., Cao, P., Chen, Y., 2022. Lactate is a key mediator that links obesity to insulin resistance via modulating cytokine production from adipose tissue. Diabetes 71, 637–652. https://doi.org/10.2337/db21-0535.

Little, T., 2015. Method validation essentials, limit of blank, limit of detection, and limit of quantitation. Biopharm Int. 28.

Liu, L., Shah, S., Fan, J., Park, J.O., Wellen, K.E., Rabinowitz, J.D., 2016. Malic enzyme tracers reveal hypoxia-induced switch in adipocyte NADPH pathway usage. Nat. Chem. Biol. 12, 345–352. https://doi.org/10.1038/nchembio.2047.

Lovejoy, J., Newby, F.D., Gebhart, S.S., DiGirolamo, M., 1992. Insulin resistance in obesity is associated with elevated basal lactate levels and diminished lactate appearance following intravenous glucose and insulin. Metab. Clin. Exp. 41, 22–27. https://doi.org/10.1016/0026-0495(92)90185-d.

Mårin, P., Rebuffé-Scrive, M., Smith, U., Björntorp, P., 1987. Glucose uptake in human adipose tissue. Metab. Clin. Exp. 36, 1154–1160. https://doi.org/10.1016/0026-0495(87)90242-3.

McNally, K., Sams, C., Loizou, G., 2019. Development, testing, parameterization, and calibration of a human physiologically based pharmacokinetic model for the plasticizer, Hexamoll® diisononyl-cyclohexane-1, 2-dicarboxylate using in silico, in vitro, and human biomonitoring data. Front. Pharmacol. 10, 1394. https://doi.org/10.3389/fphar.2019.01394.

Meeker, J.D., Sathyanarayana, S., Swan, S.H., 2009. Phthalates and other additives in plastics: human exposure and associated health outcomes. Philos. Trans. R. Soc. 364, 2097–2113. https://doi.org/10.1098/rstb.2008.0268.

NCD Risk Factor Collaboration, 2016. Trends in adult body-mass index in 200 countries from 1975 to 2014: a pooled analysis of 1698 population-based measurement studies with 19·2 million participants. Lancet 387, 1377–1396. https://doi.org/10.1016/S0140-6736(16)30054-X.

NCD Risk Factor Collaboration, 2017. Worldwide trends in body-mass index, underweight, overweight, and obesity from 1975 to 2016: a pooled analysis of 2416 population-based measurement studies in 128·9 million children, adolescents, and adults. Lancet 390, 2627–2642, 10.1016/S0140-6736(17)32129-3.

Oates, E.H., Antoniewicz, M.R., 2022. Coordinated reprogramming of metabolism and cell function in adipocytes from proliferation to differentiation. Metab. Eng. 69, 221–230. https://doi.org/10.1016/j.ymben.2021.12.005.

Pomatto, V., Cottone, E., Cocci, P., Mozzicafreddo, M., Mosconi, G., Nelson, E.R., Palermo, F.A., Bovolin, P., 2018. Plasticizers used in food-contact materials affect adipogenesis in 3T3-L1 cells. J. Steroid Biochem. Mol. Biol. 178, 322–332. https://doi.org/10.1016/j.jsbmb.2018.01.014.

Radke, E.G., Galizia, A., Thayer, K.A., Cooper, G.S., 2019. Phthalate exposure and metabolic effects: a systematic review of the human epidemiological evidence. Environ. Int. 132, 104768 https://doi.org/10.1016/j.envint.2019.04.040.

Ramirez, T., Daneshian, M., Kamp, H., Bois, F.Y., Clench, M.R., Coen, M., Donley, B., Fischer, S.M., Ekman, D.R., Fabian, E., Guillou, C., Heuer, J., Hogberg, H.T., Jungnickel, H., Keun, H.C., Krennrich, G., Krupp, E., Luch, A., Noor, F., Peter, E., Riefke, B., Seymour, M., Skinner, N., Smirnova, L., Verheij, E., Wagner, S., Hartung, T., van Ravenzwaay, B., Leist, M., 2013. Metabolomics in toxicology and preclinical research. ALTEX 30, 209–225. https://doi.org/10.14573/altex.2013.2.209.

Roberts, L.D., Virtue, S., Vidal-Puig, A., Nicholls, A.W., Griffin, J.L., 2009. Metabolic phenotyping of a model of adipocyte differentiation. Physiol. Genom. 39, 109–119. https://doi.org/10.1152/physiolgenomics.90365.2008.

Schaedlich, K., Gebauer, S., Hunger, L., Beier, L.-S., Koch, H.M., Wabitsch, M., Fischer, B., Ernst, J., 2018. DEHP deregulates adipokine levels and impairs fatty acid storage in human SGBS-adipocytes. Sci. Rep. 8, 3447. https://doi.org/10.1038/s41598-018-21800-4.

Schaffert, A., Karkossa, I., Ueberham, E., Schlichting, R., Walter, K., Arnold, J., Blüher, M., Heiker, J.T., Lehmann, J., Wabitsch, M., Escher, B.I., Bergen, M. von, Schubert, K., 2022. Di-(2-ethylhexyl) phthalate substitutes accelerate human adipogenesis through PPARγ activation and cause oxidative stress and impaired metabolic homeostasis in mature adipocytes. Environ. Int. 164, 107279 https://doi.org/10.1016/j.envint.2022.107279.

Schmeisser, S., Miccoli, A., Bergen, M. von, Berggren, E., Braeuning, A., Busch, W., Desaintes, C., Gourmelon, A., Grafström, R., Harrill, J., Hartung, T., Herzler, M., Kass, G.E.N., Kleinstreuer, N., Leist, M., Luijten, M., Marx-Stoelting, P., Poetz, O., van Ravenzwaay, B., Roggeband, R., Rogiers, V., Roth, A., Sanders, P., Thomas, R.S., Marie Vinggaard, A., Vinken, M., van de Water, B., Luch, A., Tralau, T., 2023. New approach methodologies in human regulatory toxicology - not if, but how and when. Environ. Int. 178, 108082 https://doi.org/10.1016/j.envint.2023.108082.

Schütze, A., Kolossa-Gehring, M., Apel, P., Brüning, T., Koch, H.M., 2014. Entering markets and bodies: increasing levels of the novel plasticizer Hexamoll® DINCH® in 24 h urine samples from the German Environmental Specimen Bank. Int. J. Hyg. Environ. 217, 421–426. https://doi.org/10.1016/j.ijheh.2013.08.004.

Schütze, A., Pälmke, C., Angerer, J., Weiss, T., Brüning, T., Koch, H.M., 2012. Quantification of biomarkers of environmental exposure to di(isononyl)cyclohexane-1,2-dicarboxylate (DINCH) in urine via HPLC-MS/MS. J. Chromatogr. B 895–896, 123–130. https://doi.org/10.1016/j.jchromb.2012.03.030.

Seargent, J.M., Yates, E.A., Gill, J.H., 2004. GW9662, a potent antagonist of PPARgamma, inhibits growth of breast tumour cells and promotes the anticancer effects of the PPARgamma agonist rosiglitazone, independently of PPARgamma activation. Br. J. Pharmacol. 143, 933–937. https://doi.org/10.1038/sj.bjp.0705973.

Si, Y., Shi, H., Lee, K., 2009. Impact of perturbed pyruvate metabolism on adipocyte triglyceride accumulation. Metab. Eng. 11, 382–390. https://doi.org/10.1016/j.ymben.2009.08.001.

Silva, M.J., Jia, T., Samandar, E., Preau, J.L., Calafat, A.M., 2013. Environmental exposure to the plasticizer 1,2-cyclohexane dicarboxylic acid, diisononyl ester (DINCH) in U.S. adults (2000-2012). Environ. Res. 126, 159–163. https://doi.org/10.1016/j.envres.2013.05.007.

Silveira, E.A., Mendonça, C.R., Delpino, F.M., Elias Souza, G.V., Pereira de Souza Rosa, Lorena, Oliveira, C. de, Noll, M., 2022. Sedentary behavior, physical inactivity, abdominal obesity and obesity in adults and older adults: a systematic review and meta-analysis. Clin. Nutr. ESPEN 50, 63–73. https://doi.org/10.1016/j.clnesp.2022.06.001.

Šimunović, A., Tomić, S., Kranjčec, K., 2022. Medical devices as a source of phthalate exposure: a review of current knowledge and alternative solutions. Arh. Hig. Rada. Toksikol. 73, 179–190. https://doi.org/10.2478/aiht-2022-73-3639.

S&P Global, 2021. IHS markit. Plasticizers - Chemical Economic Handbook. (S. 17-170). https://www.spglobal.com/commodityinsights/en/ci/products/plasticizers-chemical-economics-handbook.html (Accessed 14 August 2023).

Specht, I.O., Toft, G., Hougaard, K.S., Lindh, C.H., Lenters, V., Jönsson, B.A.G., Heederik, D., Giwercman, A., Bonde, J.P.E., 2014. Associations between serum phthalates and biomarkers of reproductive function in 589 adult men. Environ. Int. 66, 146–156. https://doi.org/10.1016/j.envint.2014.02.002.

Stahlhut, R.W., van Wijngaarden, E., Dye, T.D., Cook, S., Swan, S.H., 2007. Concentrations of urinary phthalate metabolites are associated with increased waist circumference and insulin resistance in adult U.S. males. Environ. Health Perspect. 115, 876–882. https://doi.org/10.1289/ehp.9882.

Tachibana, K., Kobayashi, Y., Tanaka, T., Tagami, M., Sugiyama, A., Katayama, T., Ueda, C., Yamasaki, D., Ishimoto, K., Sumitomo, M., Uchiyama, Y., Kohro, T., Sakai, J., Hamakubo, T., Kodama, T., Doi, T., 2005. Gene expression profiling of potential peroxisome proliferator-activated receptor (PPAR) target genes in human hepatoblastoma cell lines inducibly expressing different PPAR isoforms. Nucl. Recept. 3, 3. https://doi.org/10.1186/1478-1336-3-3.

Tanner, L.B., Goglia, A.G., Wei, M.H., Sehgal, T., Parsons, L.R., Park, J.O., White, E., Toettcher, J.E., Rabinowitz, J.D., 2018. Four key steps control glycolytic flux in mammalian cells. Cell Syst 7, 49–62.e8. https://doi.org/10.1016/j.cels.2018.06.003.

Tordjman, J., Chauvet, G., Quette, J., Beale, E.G., Forest, C., Antoine, B., 2003. Thiazolidinediones block fatty acid release by inducing glyceroneogenesis in fat cells. J. Biol. Chem. 278, 18785–18790. https://doi.org/10.1074/jbc.M206999200.

Trayhurn, P., 2014. Hypoxia and adipocyte physiology: implications for adipose tissue dysfunction in obesity. Annu. Rev. Nutr. 34, 207–236. https://doi.org/10.1146/annurev-nutr-071812-161156.

United States Congress, 2008. Public Law 110–314 - Consumer Product Safety Improvement Act of 2008.

Useini, A., Engelberger, F., Künze, G., Sträter, N., 2023. Structural basis of the activation of PPARγ by the plasticizer metabolites MEHP and MINCH. Environ. Int. 173, 107822 https://doi.org/10.1016/j.envint.2023.107822.

Visscher, T.L., Seidell, J.C., 2001. The public health impact of obesity. Annu. Rev. Publ. Health 22, 355–375. https://doi.org/10.1146/annurev.publhealth.22.1.355.

Völker, J., Ashcroft, F., Vedøy, Å., Zimmermann, L., Wagner, M., 2022. Adipogenic activity of chemicals used in plastic consumer products. Environ. Sci. Technol. 56, 2487–2496. https://doi.org/10.1021/acs.est.1c06316.

Vogel, N., Schmidt, P., Lange, R., Gerofke, A., Sakhi, A.K., Haug, L.S., Jensen, T.K., Frederiksen, H., Szigeti, T., Csákó, Z., Murinova, L.P., Sidlovska, M., Janasik, B., Wasowicz, W., Tratnik, J.S., Mazej, D., Gabriel, C., Karakitsios, S., Barbone, F., Rosolen, V., Rambaud, L., Riou, M., Murawski, A., Leseman, D., Koppen, G., Covaci, A., Lignell, S., Lindroos, A.K., Zvonar, M., Andryskova, L., Fabelova, L., Richterova, D., Horvat, M., Kosjek, T., Sarigiannis, D., Maroulis, M., Pedraza-Diaz, S., Cañas, A., Verheyen, V.J., Bastiaensen, M., Gilles, L., Schoeters, G., Esteban-López, M., Castaño, A., Govarts, E., Koch, H.M., Kolossa-Gehring, M., 2023. Current exposure to phthalates and DINCH in European children and adolescents - results from the HBM4EU Aligned Studies 2014 to 2021. Int. J. Hyg. Environ. 249, 114101 https://doi.org/10.1016/j.ijheh.2022.114101.

Wabitsch, M., Brenner, R.E., Melzner, I., Braun, M., Möller, P., Heinze, E., Debatin, K.M., Hauner, H., 2001. Characterization of a human preadipocyte cell strain with high capacity for adipose differentiation. Int. J. Obes. Relat. Metab. Disord. 25, 8–15. https://doi.org/10.1038/sj.ijo.0801520.

Wu, W., Li, M., Liu, A., Wu, C., Li, D., Deng, Q., Zhang, B., Du, J., Gao, X., Hong, Y., 2020. Bisphenol A and the risk of obesity a systematic review with meta-analysis of the epidemiological evidence. Dose Response 18, 1559325820916949. https://doi.org/10.1177/1559325820916949.

Xu, H.E., Lambert, M.H., Montana, V.G., Plunket, K.D., Moore, L.B., Collins, J.L., Oplinger, J.A., Kliewer, S.A., Gampe, R.T., McKee, D.D., Moore, J.T., Willson, T.M., 2001. Structural determinants of ligand binding selectivity between the peroxisome proliferator-activated receptors. Proc. Natl. Acad. Sci. U.S.A. 98, 13919–13924. https://doi.org/10.1073/pnas.241410198.